

# *Technical Review*

No. 12

## Contents

### PART I

|   |    |
|---|----|
| ● THORPEX - Pacific Asian Regional Campaign (T-PARC)  |    |
| - <a href="#">Summary</a> .....   | 1  |
| - <a href="#">DLR Falcon Dropsonde Operation in T-PARC and Analysis of the Environment Surrounding Typhoons</a> ..... | 5  |
| - <a href="#">Total Energy Singular Vector Guidance Developed at JMA for T-PARC</a> .....                             | 13 |
| - <a href="#">Observing-system Experiments Using the Operational NWP System of JMA</a> ...                            | 29 |
| - <a href="#">T-PARC Website at MRI</a> .....   | 45 |

### PART II

|  |    |
|--|----|
| ● <a href="#">JMA's Five-day Tropical Cyclone Track Forecast</a> ..... | 55 |
|--|----|

**Japan Meteorological Agency**

**March 2010**

## PREFACE

The RSMC Tokyo - Typhoon Center provides a variety of tropical cyclone information products to National Meteorological and Hydrological Services (NMHSs) on a real-time basis in order to support tropical cyclone forecasting and disaster preparedness and prevention activities. The Center also issues *RSMC Tropical Cyclone Best Track and Annual Report on the Activities of the RSMC Tokyo - Typhoon Center* every year. In addition to these regular publications, it also occasionally publishes its *Technical Review* to outline the achievements of research and development on operational meteorological services related to tropical cyclones.

This issue of *Technical Review No. 12* covers the two topics of T-PARC and five-day track forecasting. The THORPEX Pacific Asian Regional Campaign (T-PARC) was conducted in 2008 to promote better understanding of the life cycle of tropical cyclones. The comprehensive overview of the T-PARC is summarized in this issue, including aircraft observations, sensitivity analysis system and experiments on observing systems. Also featured is JMA's five-day tropical cyclone track forecast, which became operational in 2009. The method and interpretation of these forecasts are covered in detail.

The RSMC Tokyo - Typhoon Center hopes this issue will serve as a useful reference to enhance understanding of typhoon forecasting with NWP and the mitigation of typhoon-related disasters.



## THORPEX - Pacific Asian Regional Campaign (T-PARC)

**Tetsuo Nakazawa<sup>1</sup>, Kotaro Bessho<sup>1</sup>, Shunsuke Hoshino<sup>1</sup>, Takuya Komori<sup>2</sup>,  
Koji Yamashita<sup>2</sup>, Yoichiro Ohta<sup>2</sup> and Kiyotomi Sato<sup>2</sup>**

<sup>1</sup> Meteorological Research Institute

<sup>2</sup> Numerical Prediction Division, Japan Meteorological Agency

### Abstract

The THORPEX Pacific Asian Regional Campaign (T-PARC) was conducted in 2008 under an international partnership to understand the life cycle of tropical cyclones over the western North Pacific from genesis through intensification to recurvature and extra-tropical transition.

THORPEX is a ten-year international global atmospheric research project (see [http://www.wmo.int/pages/prog/arep/thorpex/index\\_en.html](http://www.wmo.int/pages/prog/arep/thorpex/index_en.html)) being implemented under the World Weather Research Programme (WWRP) of the World Meteorological Organization (WMO). Its aim is to accelerate improvements in the accuracy of one-day to two-week high-impact weather forecasts and society's utilization of weather products. The program was established by the WMO Congress at its 14th session (Geneva, May 2003).

During the T-PARC special observations period between 1 August and 5 October 2008, the Japan Meteorological Agency (JMA) deployed the following enhanced observations targeting Nuri (0812), Sinlaku (0813) and Jangmi (0815) with the aim of improving numerical weather prediction (NWP) performance for TCs: (i) enhanced upper soundings by two research vessels and four automatic upper-sounding stations, and (ii) MTSAT rapid-scan operations, in addition to collaborative dropsonde operations by the DLR Falcon. JMA also provided products related to typhoon ensemble forecasting and sensitive-area information useful for typhoon-targeting observations.

To support T-PARC's operations, JMA also created a web page at <http://tparc.mri-jma.go.jp> to give an overview of the campaign. The page includes the special-observations schedule, provides information on current atmospheric conditions and forecasts, and gives guidance on special observations and data/information for THORPEX researchers. Plans are also under way to provide special observation datasets for researchers via the page.

JMA has also conducted several studies regarding the impact of T-PARC observation data on numerical predictions of tropical cyclone tracks and intensities. One study indicated a case where special observation data had a large positive impact on tropical cyclone track forecasts for Sinlaku, but less impact on those for Jangmi.

## **1. Introduction**

In the 2008 typhoon season, an international field experiment involving special typhoon observations was carried out as part of the World Meteorological Organization (WMO) research programme.

THORPEX is a ten-year international global atmospheric research project (see [http://www.wmo.int/pages/prog/arep/thorpex/index\\_en.html](http://www.wmo.int/pages/prog/arep/thorpex/index_en.html)) being implemented under the WMO's World Weather Research Programme (WWRP). Its aim is to accelerate improvements in the accuracy of one-day to two-week high-impact weather forecasts and society's utilization of weather products. The project was established in May 2003 by the 14th WMO Congress.

As a regional THORPEX project, a summer field experiment called the THORPEX Pacific Asian Regional Campaign (T-PARC) was conducted. T-PARC is a project based on the societal needs of typhoon-prone countries in Asia, and aims to improve prediction in the following two areas: (i) the life cycle of tropical cyclones in the western North Pacific from genesis to extratropical transition/decay, and (ii) high-impact weather events over North America, the Arctic and elsewhere whose dynamical roots and/or forecast errors are driven by typhoons and other intense cyclogenesis events over east Asia and the western Pacific.

This summer field experiment had three specific major areas of focus: (i) tropical cyclogenesis, (ii) recurvature, and (iii) extra-tropical transition. The objectives of T-PARC include both the improvement of regional prediction in Asia and North America and the study of these events' impacts on the downstream flow of global atmospheric circulation.

During the T-PARC special observation period from 1 August to 5 October 2008, eleven tropical circulation systems, including four named tropical cyclones (Nuri, Sinlaku, Hagiput and Jangmi), were observed using a variety of observation tools including sondes, manned aircraft (the DLR Falcon and planes from the US Air Force in addition to aircraft from a related science project) and the MTSAT satellite. The observation data gathered provide a deeper understanding of typhoons and other high-impact weather events and help to improve related forecasting.

During the campaign, the Japan Meteorological Agency (JMA) deployed the following enhanced observations targeting Nuri (0812), Sinlaku (0813) and Jangmi (0815): (i) enhanced upper soundings by two research vessels and four land stations, and (ii) MTSAT rapid-scan operations, in addition to collaborative dropsonde operations by the DLR Falcon. The Agency also provided products related to typhoon ensemble forecasting and sensitive-area information useful for typhoon-targeting observation.

To support T-PARC's operations, JMA also created a web page at <http://tparc.mri-jma.go.jp> to give an overview of the campaign. The page includes the special-observation schedule, provides information on current atmospheric conditions and forecasts, and gives guidance on special observations and data/information for THORPEX researchers. Plans are also under way to provide special observation datasets for researchers via the page.

After the special observations, JMA conducted a preliminary study on the impact of T-PARC observation data on numerical prediction. The study indicated a case where special observations had a large positive impact on track forecasts for Sinlaku, but less impact on those for Jangmi.

## **2. Overview of the THORPEX Pacific Asian Regional Campaign**

### ***2.1 Objectives***

The main objectives of T-PARC are to understand (i) tropical cyclogenesis, (ii) recurvature of tropical cyclones, and (iii) extra-tropical transition of tropical cyclones. Each of these includes regional prediction goals for Asia and North America and studies on the impacts of these events in relation to downstream flow. To accomplish the above objectives, the following aircrafts were used:

- DLR Falcon 20
- WC-130J (from USAF under the TCS-08 program)
- P-3 (from NRL under TCS-08)
- ASTRA (from DOTSTAR)

In addition, driftsonde operation was conducted by the US, special upper-sounding operations were performed by the Korea Meteorological Administration (KMA) and JMA, and MTSAT-2 rapid-scan operations were performed by JMA.

During the campaign (1 August to 5 October 2008), eleven tropical circulation systems were observed in total. These consisted of four named tropical cyclones (Nuri, Sinlaku, Hagiput and Jangmi), one tropical depression, one ex-tropical storm and five others. Here, we give an overview of the campaign conducted by JMA.

### ***2.2 THORPEX and T-PARC***

THORPEX is a 10-year international global atmospheric research program run under the World Meteorological Organization (WMO)/World Weather Research Program (WWRP) to accelerate improvements in the accuracy of one-day to two-week high-impact weather forecasts and society's utilization of weather products.

T-PARC is based on societal needs to improve prediction of (i) the life cycle of tropical cyclones in the western Pacific from genesis to extratropical transition/decay, and (ii) high-impact weather events over North America, the Arctic and elsewhere whose dynamical roots and/or forecast errors are driven by upstream typhoons and other intense cyclogenesis events over east Asia and the western Pacific.

Scientists mainly from the Republic of Korea and Japan participated in T-PARC to understand the mechanism behind tropical cyclone recurvature and examine the feasibility of targeted observations for such cyclones. Driftsonde observation using the DLR Falcon is covered by Bessho et al. in this volume in more detail.

The targeting expert team was organized to guide aircraft flight missions involving the provision of sensitivity information near tropical cyclones using different types of sensitivity analysis, such as the singular vector method or the ensemble Kalman filter technique. A more detailed description of JMA's sensitivity analysis is given in a separate paper by Komori et al. in this volume.

### **2.3 Observation System Experiment (OSE) for Sinlaku and Jangmi**

The major concern for Japan is the impact of targeted observation on tropical cyclone track forecasting. Several Observing System Experiments (OSEs) were performed to evaluate the related impacts for Sinlaku and Jangmi, with the results indicating an overall improvement in the accuracy of track forecasting. For Sinlaku, the track forecast was improved by 20 – 30 percent for the period 0 – 12 hours before recurvature and by 10 percent in 60 – 84 hours after recurvature. However, for Jangmi, the tracks both with and without special sonde observations were identical, suggesting that the impact is small when the forecast is good. Intercomparison of track forecasts by several centers (JMA, KMA, ECMWF and NCEP) is now under way to identify common features and differences among them. More detailed information is available in a separate paper by Yamashita et al. in this volume.

### **2.4 T-PARC webpage**

Huge amounts of observation and forecast data are available from the special experiments performed under T-PARC in 2008. For researcher convenience, a number of related products from JMA and other organizations are provided on the T-PARC website at <http://tparc.mri-jma.go.jp/>. The details of the information on the webpage are described in a separate paper by Hoshino and Nakazawa in this volume.

## **3. Conclusion**

During the T-PARC special observation period from 1 August to 5 October 2008, JMA deployed the following enhanced observations targeting Nuri, Sinlaku and Jangmi to improve numerical weather prediction (NWP) performance for TCs: (i) enhanced upper soundings by two research vessels and four automatic upper-sounding stations, and (ii) MTSAT rapid-scan operations, in addition to collaborative dropsonde operations by the DLR Falcon. The Agency also provided products related to typhoon ensemble forecasting and sensitive-area information useful for typhoon-targeting observation.

JMA has also conducted several studies regarding the impact of using the T-PARC special targeted observation data on numerical predictions of tropical cyclone tracks and intensities. One study indicated a case where special observation data had a large positive impact on tropical cyclone track forecasts for Sinlaku, but less impact on those for Jangmi.

## DLR Falcon Dropsonde Operation in T-PARC and Analysis of the Environment Surrounding Typhoons

**Kotaro Bessho<sup>1</sup>, Tetsuo Nakazawa<sup>1</sup> and Martin Weissmann<sup>2</sup>**

<sup>1</sup> Meteorological Research Institute, Japan Meteorological Agency

<sup>2</sup> German Aerospace Center, Oberpfaffenhofen, Germany

### 1. DLR Falcon dropsonde operation in T-PARC

From 23 August to 4 October 2008, missions of the German Aerospace Center (DLR)'s Falcon 20-E5 aircraft (Figure 1) were executed under T-PARC in conjunction with the Meteorological Research Institute of the Japan Meteorological Agency. In terms of observational equipment, the aircraft used a dropsonde system, wind lidar, moisture profile lidar of DIAL in T-PARC. On observational flights, the Falcon was manned by two pilots, an engineer and three researchers. The plane's maximum flight range is 1,500 nautical miles (corresponding to around four hours of flight time), and its maximum flight altitude is FL390 – almost 200 hPa. Its dropsonde system, manufactured by Vaisala, has four channels in its receiver and can observe the overall atmospheric profile once every five minutes. The observational data collected by the Falcon were submitted to the WMO GTS via satellite phone through the Iridium system in the T-PARC mission. The Falcon used the US Naval Air Facility Atsugi as its main airport, and sometimes stopped at the US bases in Misawa, Iwakuni and Kadena (Figure 2) to refuel and for overnight stays.



Figure 1 The DLR Falcon 20-E5 (© The Yomiuri Shimbun)

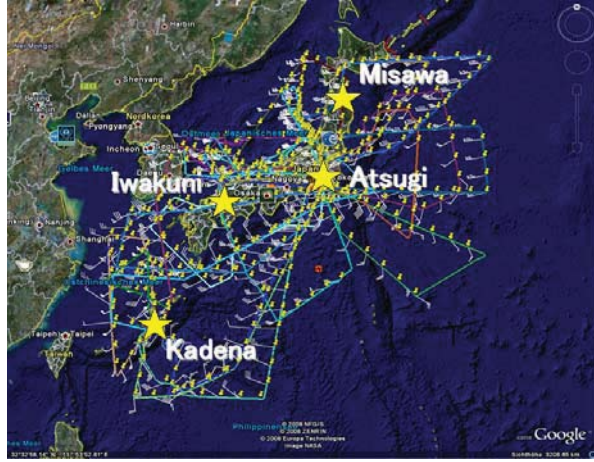


Figure 2 All Falcon flight paths in T-PARC

The Falcon observed atmospheric profiles inside and outside cloud masses surrounding typhoons using its dropsonde system, engaging in 25 missions around the Japanese islands over a total flight time of 85 hours (Table 1). The total number of dropsondes employed on these flights was 328. The observational targets were mainly the recurvatures and extratropical cyclone transitions of typhoons Sinlaku and Jangmi.

Table 1 Summary of Falcon missions in T-PARC including flight mission numbers, take-off/landing bases, start dates, flight times, block times, dropsonde numbers, mission types and target systems

| Flight | Location |          | Start Date | Flight Time |       |       |       | Block Time | Drops.   | Type        | System   |         |
|--------|----------|----------|------------|-------------|-------|-------|-------|------------|----------|-------------|----------|---------|
|        | from     | to       |            | LT          | Start | End   | UTC   |            |          |             |          |         |
| 0      | DLR OP   | DLR OP   |            |             |       |       |       | 1:30:00    | 0        | test flight | ---      |         |
| 1      | Atsugi   | Atsugi   | 2008/8/26  | 7:20        | 10:55 | 22:20 | 1:55  | 3:35:00    | 3:50:00  | 9           | T, RB    |         |
| 2      | Atsugi   | Atsugi   | 2008/8/30  | 7:10        | 10:35 | 22:10 | 1:35  | 3:25:00    | 3:40:00  | 15          | TWE, ET  | TCS25   |
| 3      | Atsugi   | Atsugi   | 2008/8/31  | 7:10        | 10:55 | 22:10 | 2:05  | 3:55:00    | 4:10:00  | 16          | TWE, ET  | TCS26   |
| 4      | Atsugi   | Atsugi   | 2008/9/2   | 7:20        | 10:50 | 22:20 | 1:50  | 3:30:00    | 3:45:00  | 17          | midlat T |         |
| 5      | Atsugi   | Atsugi   | 2008/9/4   | 6:55        | 10:35 | 21:55 | 1:35  | 3:40:00    | 3:55:00  | 15          | midlat T |         |
| 6      | Atsugi   | Atsugi   | 2008/9/9   | 7:10        | 10:50 | 22:10 | 1:50  | 3:40:00    | 3:55:00  | 18          | T, ET    | TCS37   |
| 7      | Atsugi   | Kadena   | 2008/9/11  | 12:20       | 16:20 | 3:20  | 7:20  | 4:00:00    | 4:00:00  | 19          | Typhoon  | Sinlaku |
| 8      | Kadena   | Atsugi   |            | 17:15       | 21:20 | 8:15  | 12:20 | 4:05:00    | 4:20:00  | 17          | Typhoon  | Sinlaku |
| 9      | Atsugi   | Iwa-Kuni | 2008/9/14  | 8:30        | 12:45 | 23:30 | 3:15  | 3:45:00    | 4:00:00  | 22          | Typhoon  | Sinlaku |
| 10     | Iwa-Kuni | Atsugi   |            | 13:45       | 14:55 | 4:45  | 5:55  | 1:10:00    | 1:25:00  | 0           | Typhoon  | Sinlaku |
| 11     | Atsugi   | Kadena   | 2008/9/16  | 6:35        | 10:20 | 21:35 | 1:20  | 3:45:00    | 4:00:00  | 17          | Typhoon  | Sinlaku |
| 12     | Kadena   | Atsugi   |            | 14:00       | 17:00 | 5:00  | 8:00  | 3:00:00    | 3:50:00  | 3           | Typhoon  | Sinlaku |
| 13     | Atsugi   | Iwa-Kuni | 2008/9/17  | 12:20       | 15:35 | 3:20  | 6:35  | 3:15:00    | 3:30:00  | 17          | ET       | Sinlaku |
| 14     | Iwa-Kuni | Atsugi   |            | 16:50       | 20:15 | 7:50  | 11:15 | 3:25:00    | 3:40:00  | 15          | ET       | Sinlaku |
| 15     | Atsugi   | Atsugi   | 2008/9/18  | 12:25       | 16:20 | 3:25  | 7:20  | 3:45:00    | 4:10:00  | 16          | ET       | Sinlaku |
| 16     | Atsugi   | Misawa   | 2008/9/19  | 7:35        | 8:55  | 22:35 | 23:55 | 1:20:00    | 1:35:00  | 3           | ET       | Sinlaku |
| 17     | Misawa   | Atsugi   |            | 10:10       | 14:10 | 1:10  | 5:10  | 4:00:00    | 4:15:00  | 19          | ET       | Sinlaku |
| 18     | Atsugi   | Atsugi   | 2008/9/21  | 7:05        | 11:05 | 22:05 | 2:05  | 4:00:00    | 4:15:00  | 12          | ET       | Sinlaku |
| 19     | Atsugi   | Kadena   | 2008/9/28  | 12:10       | 16:00 | 3:10  | 7:00  | 3:50:00    | 4:05:00  | 13          | Typhoon  | Jangmi  |
| 20     | Kadena   | Kadena   |            | 17:45       | 19:50 | 8:45  | 11:10 | 2:25:00    | 2:40:00  | 9           | Typhoon  | Jangmi  |
| 21     | Kadena   | Kadena   | 2008/9/29  | 12:45       | 16:15 | 3:45  | 7:15  | 3:50:00    | 4:05:00  | 10          | Typhoon  | Jangmi  |
| 22     | Kadena   | Atsugi   | 2008/9/30  | 7:10        | 10:40 | 22:10 | 1:40  | 3:30:00    | 3:45:00  | 12          | ET, T    | Jangmi  |
| 23     | Atsugi   | Atsugi   |            | 12:55       | 17:50 | 3:55  | 8:50  | 3:55:00    | 4:10:00  | 8           | ET, T    | Jangmi  |
| 24     | Atsugi   | Iwa-Kuni | 2008/10/1  | 14:15       | 17:30 | 5:15  | 8:30  | 3:15:00    | 3:30:00  | 16          | ET       | Jangmi  |
| 25     | Iwa-Kuni | Atsugi   |            | 19:45       | 22:30 | 10:45 | 13:30 | 2:45:00    | 3:00:00  | 10          | Typhoon  | Jangmi  |
|        |          |          |            |             |       |       |       | 84:45:00   | 93:00:00 | 328         |          |         |

Three other aircraft were used on T-PARC missions, including the USAF Hurricane Hunters WC-130 and the NRL P-3. Since the main targets of these two planes were typhoon genesis and recurvature, they used Guam as their main airport. The other aircraft was the DOTSTAR program's Astra, which flew near Taiwan Island to cover the typhoon recurvature stage. All three were equipped with dropsonde systems to enable atmospheric profiling in areas near typhoons. In particular, the WC-130 also sometimes executed eye-wall penetration flights. The total number of flight hours logged in T-PARC by the four aircraft including the Falcon was more than 500 over 76 missions.

## 2. Autumn rain front and typhoons

In late summer and early autumn, the Autumn Rain Front (ARF) approaches the Japanese islands. The ARF is similar to the Baiu-Meiyu-Chagma front in early summer, but usually it brings light rain rather than the heavy rainfall of the Baiu front. It is usually located near the Japanese islands with an east-west orientation, and sometimes causes major disasters such as flash flooding in combination with typhoons moving to mid-latitude areas. By way of example, the torrential rain in the Tokai region observed in Nagoya City (located in the central part of Japan's main island) from 11 to 12 September 2000 was caused by interaction between the ARF and Typhoon Saomai (0014) (Kitabatake 2002).

As mentioned above, the combination of the ARF with typhoon conditions sometimes brings major disasters to the Japanese islands. Many field experiments and research projects have been carried out in regard to the Baiu front, and special observations of it prove successful if the monitoring period is long enough. However, there has been a lack of research involving observational experiments for the ARF because of the extreme difficulty and risk involved in capturing the rare cases of heavy ARF rainfall in combination with typhoons. In T-PARC, the Falcon had many chances for detailed observation of ARF structures under the influence of typhoons. In such conditions, the ARF may produce extensive latent heat release, thereby changing the structure of the typhoon itself. Accordingly, it is very important to analyze such fronts observationally. In the next section, typical results of ARF observation from a Falcon dropsonde mission will be shown to allow analysis of the environmental structure of typhoons.

## 3. ARF case study

Below are some results of observing the ARF under the influence of a typhoon approaching the Japanese islands. Figure 3 is a JMA surface weather map made with data from 00 UTC on 16 September 2008. From this figure, it can be understood that Typhoon Sinlaku (0813) was positioned north of Taiwan Island, with the ARF located along the southern coast of Japan's main islands. Figure 4 shows an MTSAT infrared satellite image taken at the same time as the data used for the weather map. The red dots with numbers represent the dropsonde observational points of the Falcon, and the yellow stars show the two JMA operational upper-sounding sites used in the analysis.

Dropsonde observation was executed from 2207 UTC on 15 September to 0106 UTC on 16 September. Figure 5 shows a rain intensity image for the area over the Japanese islands retrieved from JMA's operational radars at 2200 UTC on 15 September. From these figures, it can be seen that the dropsonde observational points and JMA's upper-sounding sites were located over the ARF in a north-to-south direction.

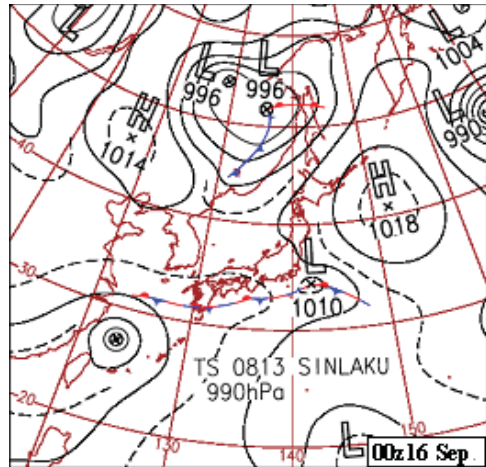


Figure 3 JMA surface weather map for 00 UTC on 16 September 2008

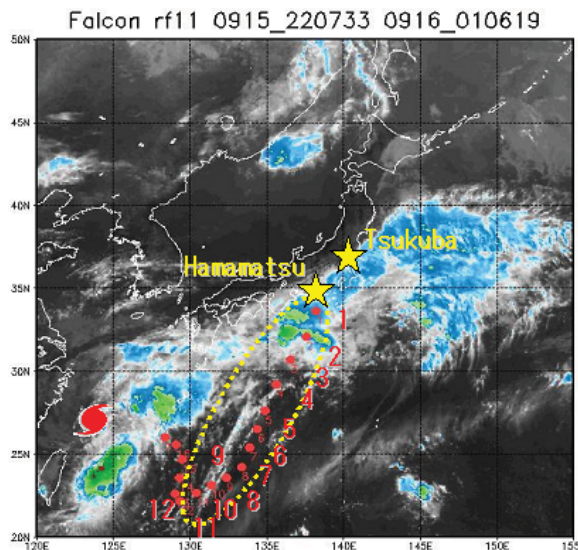


Figure 4 Infrared image from MTSAT-1R at 00 UTC on 16 September 2008. The red dots show Falcon dropsonde observational points, and the yellow stars indicate the JMA operational upper-sounding sites used in the analysis.

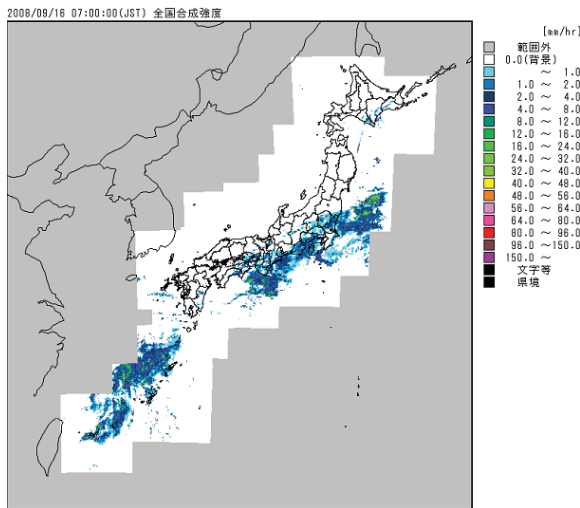


Figure 5 Rain intensity (mm/hr) as retrieved from JMA operational radars at 2200 UTC on 15 September 2008

Figure 6 shows cross sections derived from atmospheric profiles of dropsondes #1 – 12 and two operational soundings at Tsukuba and Hamamatsu. Tsukuba was located to the north of the ARF, Hamamatsu and dropsondes #1 – 3 were located within it, and dropsondes #4 – 12 were to its southern side. Figures 6 (a), (b) and (c) show cross sections of potential temperature, specific humidity and equivalent potential temperature, respectively, with each indicating the same cross section of horizontal wind. In this case study, the lower structure of the ARF below 950 hPa was the point of focus.

At Tsukuba, the horizontal wind had an easterly component, but it was very weak at a lower level. At Hamamatsu, the wind speed showed a sudden increase to almost 10 m/s. The horizontal wind at dropsonde #1 had almost the same speed, but its direction was northeasterly. Unfortunately, no wind data were obtained from dropsonde #2. At dropsonde #3 located to the southern edge of the ARF, the wind speed was 5 m/s and its direction was southwesterly. From the wind speeds and directions between dropsondes #1 and #3, it can be easily inferred that there is a strong convergence within the ARF at a lower level. Wind data for dropsondes #4 and #5 are also missing. At dropsonde #6, the wind speed was almost 5 m/s, and its direction was southeasterly. The horizontal winds at dropsondes #7 – 12 were very weak (below 700 hPa).

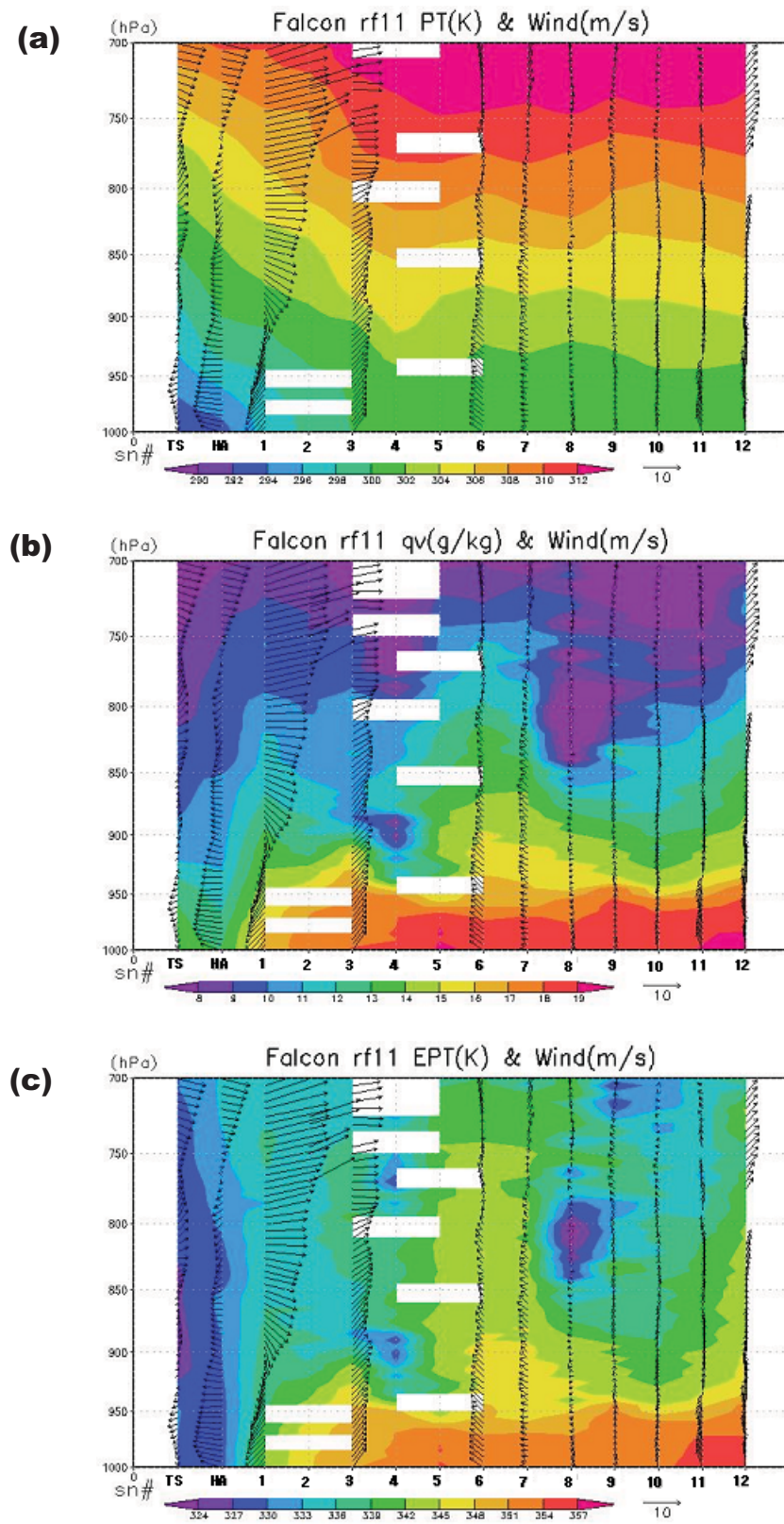


Figure 6 Cross sections derived using atmospheric profiles from dropsondes #1 – 12 and two operational soundings at Tsukuba (TS) and Hamamatsu (HA). (a) Potential temperature (K); (b) specific humidity (g/kg); (c) equivalent potential temperature (K). (a) – (c) also include horizontal wind vectors (m/s).

For the potential temperature profile at the lowest level, there was a significant gradient between Tsukuba and dropsonde #3 corresponding to the ARF itself (Figure 6 (a)). The gradient of potential temperatures below 950 hPa over the southern side of the ARF was very small, while the horizontal distribution of specific humidity showed a large gradient between Tsukuba and dropsonde #4 (Figure 6 (b)). Reflecting the distribution of potential temperature and specific humidity at the lowest level, the horizontal gradient of equivalent potential temperature at this level between Hamamatsu and dropsonde #4 was very large, and the level of stability over these areas was almost neutral (Figure 6 (c)). On the other hand, the gradient of equivalent potential temperature between dropsondes #4 and #10 was very weak, and the equivalent potential temperature was high at the lowest level and low above 950 hPa. This indicates that the southern side of the ARF was in a state of convective instability. In conclusion, it was found that the southern side of the ARF was characterized by a horizontal atmospheric structure with a small gradient of potential temperature and a large gradient of specific humidity.

This structure of the southern ARF appears to be similar to that of the Baiu front as found by Moteki et al. (2006), who executed dropsonde observation using aircraft on the Baiu front and showed a strong temperature gradient within the front itself and a strong humidity gradient over its southern side. In their paper, this strong moisture gradient was called a water vapor front. From our analysis, it can be concluded that there is also a water vapor front over the southern side of the ARF, which has a structure similar to that of the Baiu front.

## References

- Kitabatake, N., 2002: The role of convective instability and frontogenetic circulation in the torrential rainfall in the Tokai District on 11-12 September 2000. *Pap. Met. Geophys.*, **53**, 91-108 (in Japanese).
- Moteki, Q., T. Shinoda, S. Shimizu, S. Maeda, H. Minda, K. Tsuboki and H. Uyeda, 2006: Multiple Frontal Structures in the Baiu Frontal Zone Observed by Aircraft on 27 June 2004. SOLA, **2**, 132-135.



# Total Energy Singular Vector Guidance Developed at JMA for T-PARC

**Takuya Komori**

Numerical Prediction Division, Japan Meteorological Agency

**Ryota Sakai**

River Office, Osaka Prefectural Government

**Hitoshi Yonehara**

Numerical Prediction Division, Japan Meteorological Agency

**Takashi Kadowaki**

Numerical Prediction Division, Japan Meteorological Agency

**Kiyotomi Sato**

Numerical Prediction Division, Japan Meteorological Agency

**Takemasa Miyoshi**

University of Maryland

**Munehiko Yamaguchi**

Numerical Prediction Division, Japan Meteorological Agency

(Present affiliation: Rosenstiel School of Marine and Atmospheric Science, University of Miami)

## Abstract

A sensitivity analysis system was developed at the Japan Meteorological Agency (JMA), using a singular vector (SV) method with a moist total energy (TE) metric at both the initial and final times, to provide daily realtime guidance for the targeted observations in the THORPEX Pacific Asian Regional Campaign (T-PARC) period from August through early October of 2008. For effective decision making regarding the targeted observations for tropical cyclones (TCs), a lead time of at least two days was needed for each observation. The product with a one-day lead time was also required to refine judgment for the execution and location of the special observations. Accordingly, two types of sensitivity analysis were performed using two forecast fields ( $T+24h$  and  $T+48h$ ) of the operational

Global Spectral Model (GSM) at a resolution of TL959L60<sup>1</sup>. For the daily sensitivity analysis three common fixed target areas were specified among the guidance providers to enable inter-comparison of the sensitivity guidance in each of their calculations. JMA also conducted further sensitivity analysis using an adaptive target area in the vicinity of the TC location, because such an area is preferable when targeting a TC. Some target observations demonstrated significant impacts for operational TC track forecasts. On the other hand, a number of common and different features were found among SV guidance providers in realtime intercomparison during the T-PARC period. Some extra experiments for the case of the recurring TC revealed that differences in moist processes in the tangent linear and adjoint (hereafter TL/AD) model can explain the distinct features to a certain extent. The results highlighted a number of features of SV sensitivities.

## 1. Introduction

From August through early October of 2008, as part of THORPEX Observing-system Research and Predictability Experiment (THORPEX) framework, JMA conducted the THORPEX Pacific Asian Regional Campaign (T-PARC) project (Komori et al. 2009, Yamashita et al. 2009) in collaboration with other nations and projects (Wu et al. 2007, Elsberry and Harr 2008, Reynolds et al. 2009b, and Kim et al. 2010). T-PARC was a multi-national and multi-institution field campaign designed to enhance understanding of the mechanism behind TCs and improve forecast skill for them, in particular as a demonstration of the Global Interactive Forecast System (GIFS) - a major THORPEX objective. While the T-PARC project encompassed many objectives, JMA's major focus was on TC track forecasting, especially in the recurvature stage. This is because recurring TCs have large forecast uncertainty, and better forecasting skills are of great importance to people living in Pacific basin countries, including Japan, from the perspective of natural disaster reduction and mitigation.

With the aim of supporting the field campaign and the GIFS, monitoring was performed in regard to information on daily forecast uncertainty and the ensemble spread of TC track forecasts, provided by the operational Typhoon Ensemble Prediction System (TEPS) (Yamaguchi and Komori 2009, Yamaguchi et al. 2009) and the one-Week Ensemble Prediction System (WEPS) (Sakai et al. 2008). JMA also provided TC tracks derived from the operational GSM, TEPS (4 times a day, 11 members) and WEPS (once a day, 51 members) to science committees in real-time. The format used was Cyclone XML (CXML; more detailed information is available at: <http://www.bom.gov.au/bmrc/projects/THORPEX/TC/index.html>). Currently, CXML files are exchanged through the archive centers of the THORPEX Interactive Grand Global Ensemble (TIGGE) project.

During the project, the special observations were conducted, including dropsonde deployment by a manned Falcon aircraft, enhanced radiosonde observations by research vessels and fixed observation stations, and MTSAT rapid-scan operations (Bessho et al. 2010). Figure 1 illustrates the locations of the supplemental observations (except MTSAT rapid-scan) for all TCs during the T-PARC period. These were referred to as targeted observations because they were performed in

---

<sup>1</sup> We use T as an abbreviation for triangular truncation with a Gaussian grid, TL for triangular truncation with a linear Gaussian grid, and L for vertical layers. TL959L60 therefore denotes spectral triangular truncation at a wave number of 959 with a linear Gaussian grid and 60 vertical layers.

consideration of sensitive areas where additional atmospheric observations were assimilated to improve the analysis field and thereby reduce forecast uncertainty (Aberson 2003, Langland 2005). Most of the data were distributed in real time through the Global Telecommunication System (GTS) to enable their use in operational numerical weather prediction (NWP) systems worldwide. The efficacy of the targeted observations is discussed in an accompanying paper (Yamashita and Ohta 2010).

In support of these observations, many institutions provided information on sensitive areas as guidance using a wide variety of methods as following:

- 1) Singular Vector (SV) method from JMA (Komori et al. 2009), ECMWF, the NRL global model (Reynolds et al. 2009b) and Yonsei University (Kim et al. 2010)
- 2) Ensemble Transform Kalman Filter (ETKF) method from UKMO and the University of Miami/National Centers for Environmental Prediction (NCEP)
- 3) Adjoint-Derived Sensitivity Steering Vector (ADSSV) method from National Taiwan University (Wu et al. 2007)
- 4) Ensemble-based sensitivity method from the University of Washington
- 5) Adjoint sensitivity method from the NRL Coupled Ocean/Atmosphere Mesoscale Prediction System (COAMPS) (Reynolds et al. 2009b).

These products were compared on the website in real time, and were discussed at daily planning meetings on the web.

The purpose of this paper is to describe the product features of the JMA sensitivity analysis system implemented for the T-PARC project using an SV method with a moist total energy (TE) norm. Section 2 describes the specifications, Section 3 outlines the performance and product features, and Section 4 provides a summary.

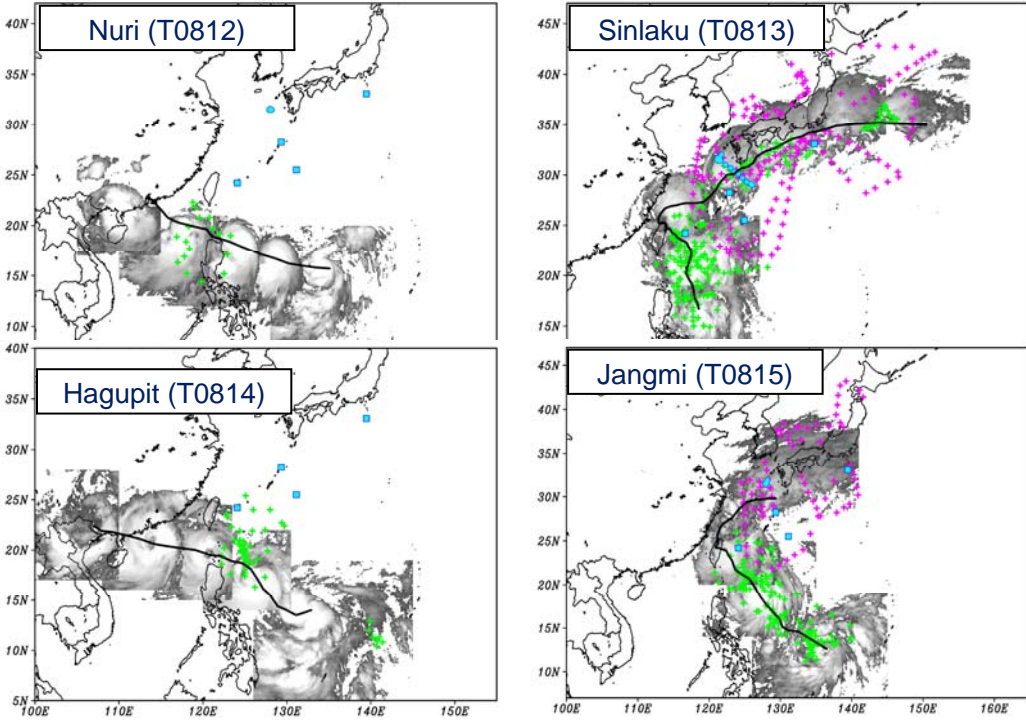


Figure 1 Schematic maps of the supplemental observational points. The best tracks of the RSMC Tokyo - Typhoon Center for each typhoon are shown by the black lines. Extra observation points for upper-soundings by JMA research vessels and ground observatories (blue points), dropsondes released by the Falcon aircraft (pink) and those released by other planes (green) are overlaid on the sensitive area.

## 2. Specifications

Using the moist SV method with a moist TE norm (Barkmeijer et al. 2001), JMA provided daily sensitivity guidance for the targeted observations conducted during the T-PARC period. The SV method can emphasize dynamical perturbation with a rapid growth rate from small initial-condition uncertainties during an optimization time interval (OTI), and has been implemented as a perturbation generator to calculate initial perturbation growth using the TL/AD model at a resolution of T63L40 for the global domain in JMA's operational TEPS and WEPS. The configuration of the moist TE norm at the initial and final times, evaluating the growth rate of perturbations, is the same as TEPS except for the initial field and target areas. The equation for the norm is as follows:

$$\begin{aligned}
 (x, \mathbf{Ex}) = & \frac{1}{2} \int_0^1 \int_S (\nabla \Delta^{-1} \zeta_x \cdot \nabla \Delta^{-1} \zeta_x + \nabla \Delta^{-1} D_x \cdot \nabla \Delta^{-1} D_x \\
 & + g(\Gamma_d - \Gamma)^{-1} \frac{T_x T_x}{T_r} \\
 & + w_q \frac{L_c^2}{c_p T_r} q_x q_x) dS \left( \frac{\partial p}{\partial \eta} \right) d\eta \\
 & + \frac{1}{2} \int_S \frac{R_d T_r}{P_r} P_x P_x dS
 \end{aligned} \tag{1}$$

where  $\zeta_x$ ,  $D_x$ ,  $T_x$ ,  $q_x$  and  $P_x$  are the vorticity, divergence, temperature, specific humidity and surface pressure components of vector  $x$ , respectively, and  $\mathbf{E}$  represents a norm operator. Note that the temperature lapse rate  $\Gamma$  is taken into consideration as an available potential energy term (Lorenz, 1955).  $c_p$  is the specific heat of dry air at a constant pressure,  $L_C$  is the latent heat of condensation, and  $R_d$  is the gas constant for dry air.  $T_r = 300$  K is a reference temperature,  $Pr = 800$  hPa is a reference pressure, and  $w_q$  is a constant ( $w_q = 1$  for the moist TE norm and  $w_q = 0$  for the dry TE norm). A representative value of  $2/3\Gamma_d$  is used for  $\Gamma$ . In Eq. (1), the vertical integration of the kinetic energy term and the available potential energy term is calculated beneath the 26th model level (around 100 hPa), and the specific humidity term is limited to the 15th model level (around 500 hPa).

To enable planning for the special targeted observations, information on the sensitivity area at the time of observation was needed at least two days in advance. The product with a one-day lead time was also required to refine judgment for the execution and location of the special observations. Accordingly, two types of sensitivity guidance were computed using two forecast fields ( $T + 24$  h and  $T + 48$  h), made by high-wavenumber truncation for the operational GSM, at a resolution of TL959L60. For the daily sensitivity analysis, three common fixed target areas (referred to as GUAM, TAIWAN and JAPAN) were specified among the guidance providers to enable inter-comparison of the sensitivity guidance in each of their calculations. These areas were utilized to support not only recurving TCs, but also TCs in the generation and extratropical transition (ET) stages. JMA also conducted further sensitivity analysis using an adaptive target area (referred to as MVTY) in the vicinity of the TC location because such an area is preferable when targeting a TC (Figure 2). When a TC was analyzed by the Regional Specialized Meteorological Center (RSMC) Tokyo - Typhoon Center, the MVTY target area was automatically defined according to the TC position forecasted by the operational GSM.

The OTIs of SVs for the GUAM, TAIWAN and JAPAN regions were also common, with the value chosen as 48 hours. Reynolds and Rosmond (2003) showed the legitimacy of OTIs from 24 hours to 72 hours for synoptic scale dynamics under the assumption of linearity, especially in the case of dry SVs. As for moist processes in JMA's TL/AD model, both large-scale cloud and deep convection schemes were implemented. As discussed in previous studies (e.g. Coutinho et al. 2004, Hoskins and Coutinho 2005), the higher growth rates of moist SVs make it preferable to use a shorter time, for which the perturbation linearity assumption is more likely to be valid. Accordingly, an OTI of 24 hours was adopted for SVs in the MVTY target area. The area size of MVTY was determined based on the statistical TC position error forecasted by the operational GSM ( $T + 24$  h and  $T + 48$  h). The specifications of JMA's sensitivity analysis for T-PARC are shown in Table 1.

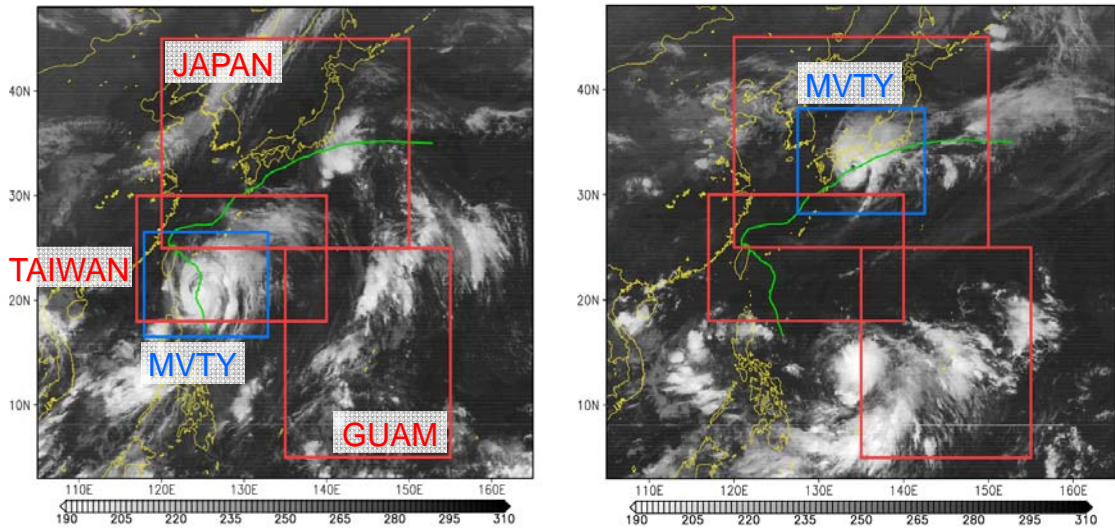


Figure 2 Schematic maps showing the four target areas (defined in Table 1) overlaid on MTSAT IR images from 00 UTC on 11 September (left) and 19 September (right) 2008. The best track of typhoon Sinlaku is shown by the green lines.

Table 1 Specifications of JMA's sensitivity analysis system for T-PARC

|                              |  |                                 |                                |          |
|------------------------------|--|---------------------------------|--------------------------------|----------|
| Forecast domain              | Global   |                                 |                                |          |
| Initial time                 | 00 UTC   |                                 |                                |          |
| Initial field with lead time | 24 hour/48 hour forecast field by operational GSM at a resolution of TL959L60                    |                                 |                                |          |
| Method                       | Singular vector  |                                 |                                |          |
| Inner model resolution       | Spectral triangular truncation at a wave number of 63 (T63), 40 levels (from surface to 0.4 hPa) |                                 |                                |          |
| Norm                         | Moist total energy   |                                 |                                |          |
| Target area                  | GUAM<br>(05–25N,<br>135–155E)  | TAIWAN<br>(18–30N,<br>117–140E) | JAPAN<br>(25–45N,<br>120–150E) | *MVTY    |
| Optimization time interval   | 48 hours   |                                 |                                | 24 hours |
| Physical process             | **Full physics   |                                 |                                |          |

\*The MVTY target area is automatically defined in the vicinity of each TC position forecasted by the operational GSM. The area is specified as 10 deg. x 10 deg. for the 24-hour forecast field and 15 deg. x 10 deg. for the 48-hour forecast field, based on the statistical TC position error of the operational GSM.

\*\*Full physics: Initialization, horizontal diffusion, surface turbulent diffusion, vertical turbulent diffusion, gravity wave drag, long wave radiation, large-scale cloud and deep convection

### 3. Performance

#### 3.1 Case studies of sensitivity guidance

Among the four TCs in Figure 1, Typhoon Sinlaku (the 13th named TC in the western North Pacific of 2008) had an especially great impact on Japan with its recurvature, reintensification and extratropical transition. In the early recurvature stage, the analysis field had a high level of uncertainty associated with the large spread for the track forecast in the operational TEPS and WEPS. Accordingly, collaborative targeted observations were planned with other institutions at daily meetings. Figure 3 (a) shows an MTSAT IR image and the observational locations from around 00 UTC on 11 September 2008. The locations were comprehensively decided based on the sensitivity guidance produced by a number of institutions. Additionally, Figure 3 shows JMA's sensitivity guidance for the MVTY target region, a vertically integrated total energy (TE) representation of the leading SV normalized by the maximum value of TE in the global domain with a two-day lead time (b) and a one-day lead time (c). These results indicate useful cases because the sensitivity guidance calculated from the analysis field (Figure 3 (d)) indicates analogous characteristics in comparison with those computed from forecast fields (Figures 3 (b) and (c)). The value of the similarity index (Buizza 1994) between the leading SVs computed from the two-day forecast field and that of the analysis field is 0.85, indicating good usability for guidance provided in advance (Komori et al. 2009).

Figure 4 (a) shows large precipitable water along with strong winds and convergence to the east of Sinlaku. The 500-hPa field of the final SV for the MVTY target area (Figure 4 (b)) has large heat release and vorticity to the northeast of Sinlaku. Such vorticity may have caused a change in the typhoon's location. The extra experiments in Section 3.2 also outline the important role of deep convection in this mechanism. The nonlinear evolved perturbation (Figure 4 (c)) from the initial SV shows a structure similar to that of the linearly evolved final SV, indicating the legitimacy of the linearity assumption in calculating the SV.

Figure 5 represents sensitivity guidance computed for three fixed target areas with different locations and sizes (TAIWAN, GUAM and JAPAN) at the same time, and shows the dependency of the SV structure on the target areas. The superimposed analysis stream lines in Figure 5 (a) indicate that the sensitivity locations emphasized by the leading SV are influenced by the mid-latitude upstream trough, a subtropical high-pressure system and the TC's surrounding flows. These figures also illustrate that the MVTY adaptive target area with a 24 h OTI (Figure 3 (b)) seems to be preferable to the fixed target areas with a 48 h OTI (Figures 5 (a), (b) and (c)) to detect sensitive areas efficiently in the vicinity of the TC. These results are due to the longer (48h) OTI and the higher-latitude target areas, which make it easier to capture the influence of the mid-latitude trough. The results are consistent with those of Komori and Kadowaki (2010).

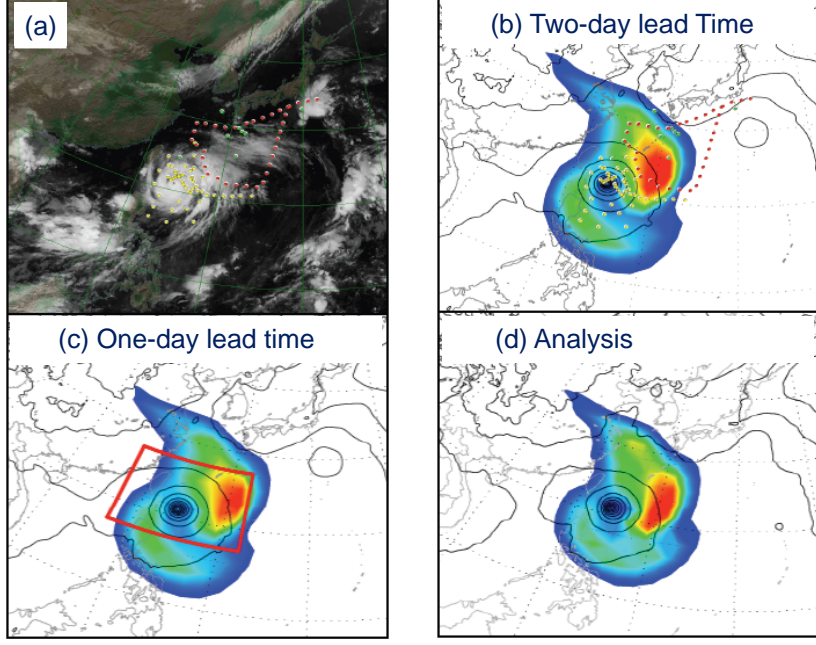


Figure 3 The leading SVs for the MVTY target area computed from (b) the two-day forecast, (c) the one-day forecast and (d) the analysis field at 00 UTC on 11 September 2008. The observation points of upper-soundings by JMA research vessels and ground observatories (green points), dropsondes released by the Falcon aircraft (red) and those released by other planes (yellow) are plotted (a) on the MTSAT image and (b) on the sensitive area.

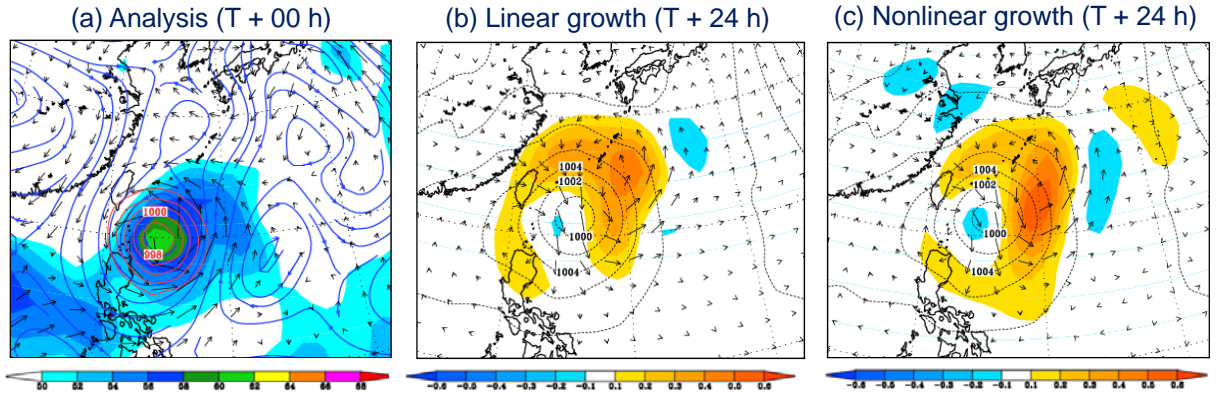


Figure 4 The sea level pressure (contour) and wind fields at 500 hPa for (a) the analysis field at a resolution of T63L40, (b) the final SV (linear growth of the initial SV) for the MVTY target area and (c) the nonlinear perturbation evolved 24 hours from the initial SV (shown in Figure 3 (d)). The shaded areas represent (a) total precipitable water vapor in each column, and (b)/(c) temperature perturbation. The 500-hPa stream lines (blue) are superimposed on the analysis field.

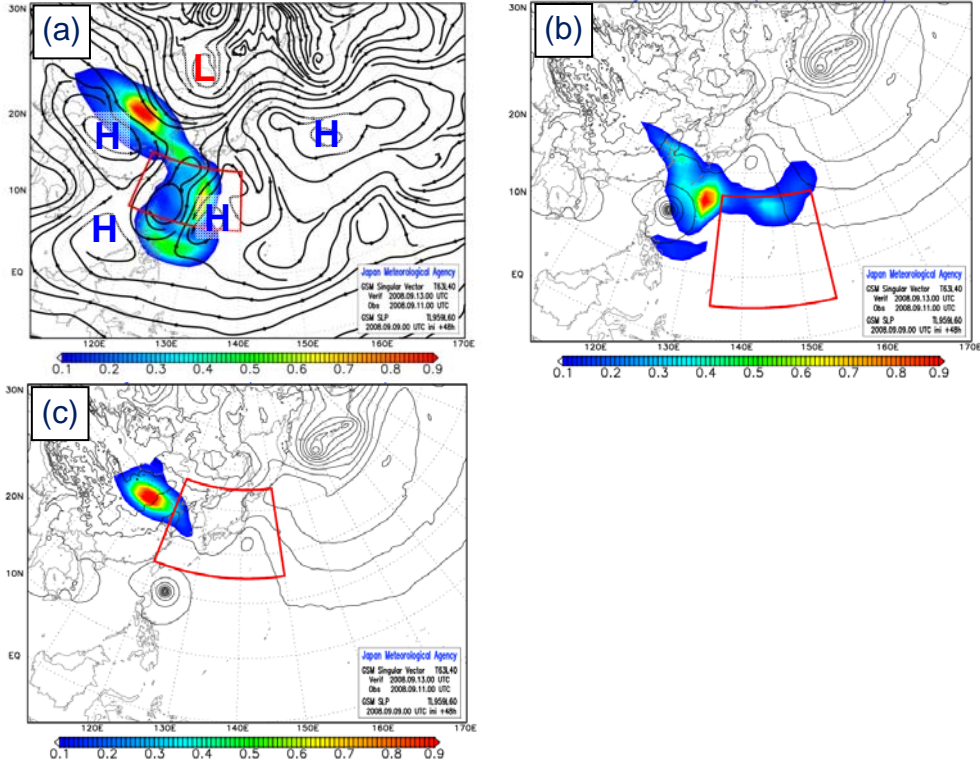


Figure 5 As per Figure 3 (b), but for the fixed target areas of (a) TAIWAN, (b) GUAM and (c) JAPAN. The stream lines at 500 hPa (a) and the surface pressure of the analysis field (b)/(c) are superimposed.

### 3.2 Impact of moist processes in the TL/AD model

Section 3.1 demonstrated the dependence of SVs in terms of 1) the location and size of the target area, 2) the OTI used to specify the growth period, and 3) the performance of the inputted analysis or forecast field. It is also well known that SVs depend on the selection of other specifications: 4) the metric and associated norm at the initial and final times, 5) the physical and dynamical processes in the TL/AD model, and 6) the resolution of the TL/AD model. Many researchers have focused on SV inter-comparison (Majumdar et al. 2006, Reynolds et al. 2007, and Wu et al. 2009) and on recurring TCs with a local target area (Peng and Reynolds 2006, Kim and Jung 2009, Chen et al. 2009 and Reynolds et al. 2009a), discussing SV features and the important role of upstream mid-latitude troughs, subtropical ridges and the flows surrounding TCs with several configurations.

In the T-PARC project, real-time inter-comparison of sensitivity analysis was performed on the website, offering comprehensive information on sensitive areas as guidance for effective decision-making related to target observations in the vicinity of a TC. However, sensitivity guidance providers using the SV method (such as JMA, ECMWF, NRL and Yonsei University) had different configurations, especially the norm, the moist processes and the resolution of the TL/AD model, causing the features of the guidance to vary in some cases. The SV dependence for the recurring Sinlaku with the resolution of the TL/AD model was investigated by Komori and Kadowaki (2010).

The present study therefore includes some extra experiments for the case of the recurving Sinlaku to investigate the impact of the norm and moist processes in the TL/AD model.

Figure 6 shows the results of these extra experiments, indicating the sensitivity guidance computed from the two-day forecast field valid at 00 UTC on 11 September 2008. In the T-PARC project, a moist SV with a moist TE norm was applied (Figures 6 (a) and (b)), which is the same configuration as the operational TEPS. In the “dry” norm, the water vapor component was set to zero. Figures 6 (c) and (d) illustrate that without a water vapor effect in the norm, the sensitive area, influenced by the confluence to the east of Sinlaku and the upstream mid-latitude trough, becomes relatively weak compared with the south side of Sinlaku. These trends are outstanding in the dry SV, having no convection and large-scale cloud scheme, with a dry TE norm (Figures 6 (e) and (f)). Hence, further experiments were performed to divide the effects of convection and the large-scale cloud scheme in the TL/AD model (Figure 7). The results show that the convection scheme in the model played a more important role than the large-scale cloud scheme in the feature of vertically integrated TE in the T-PARC project, supporting the mechanism by which the moisture convergence and associated convection caused heat release in the eastern confluence location of Sinlaku (Figure 4). Furthermore, analysis of the TIGGE ensemble data set indicates a large spread in the strength of the subtropical high pressure system (not shown), which also supports the high sensitivity in the confluence area between Sinlaku and the subtropical high pressure system.

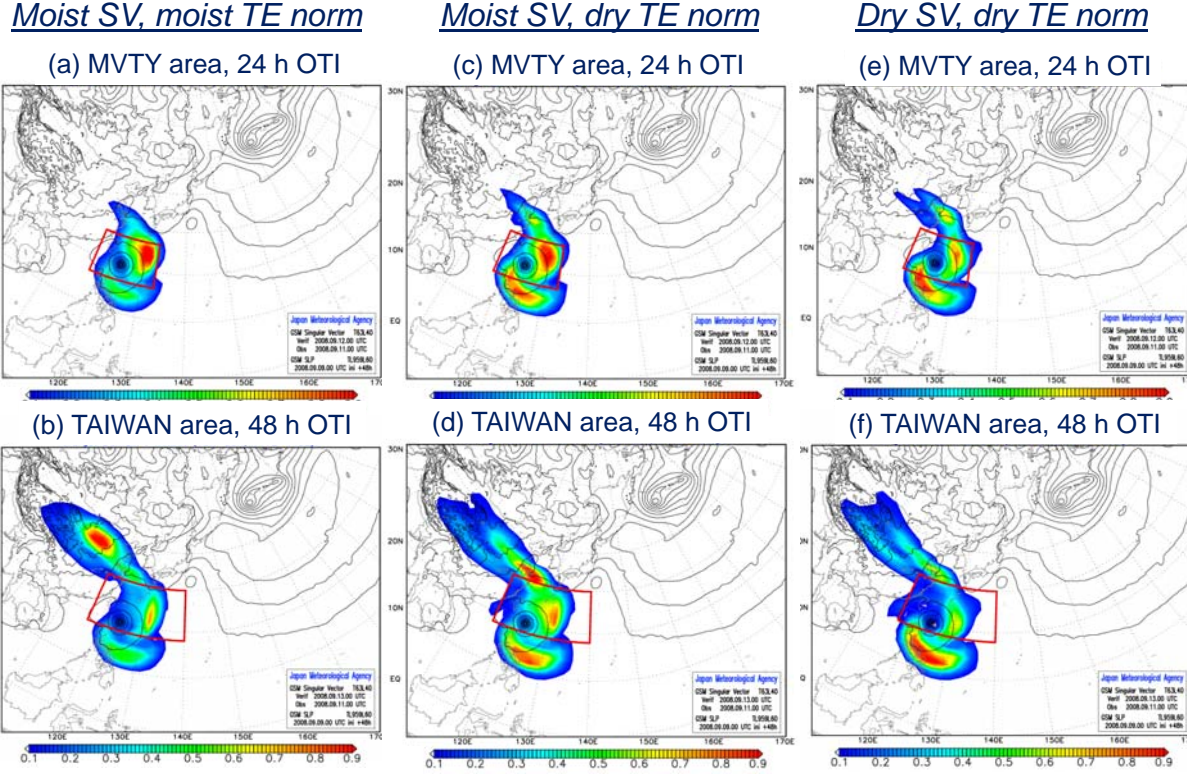


Figure 6 The vertically integrated TE of the leading SV computed from the two day forecast field, valid at 00 UTC on 11 September 2008 with different configurations of moist processes in the TL/AD model and norm: (a), (b): moist SV with a moist TE norm; (c), (d): moist SV with a dry TE norm; (e), (f): dry SV with a dry TE norm. The target area and OTI were specified as: (a), (c), (e): MVTY area with a 24-hour OTI; and (b), (d), (f): TAIWAN area with a 48-hour OTI.

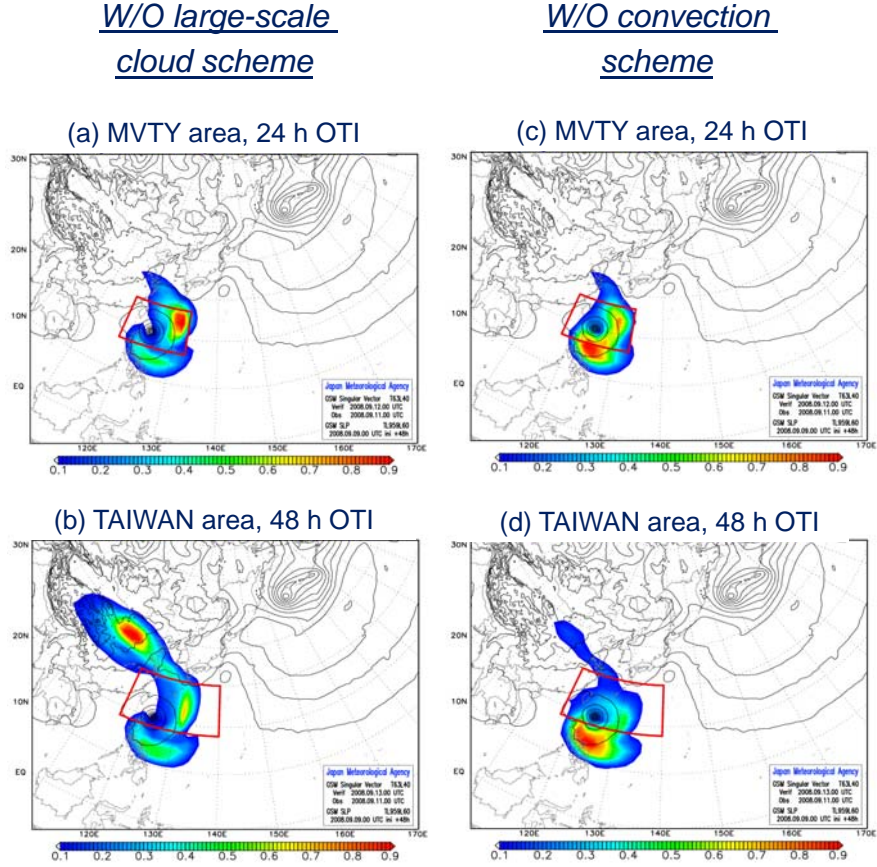


Figure 7 As per Figures 6 (a) and (b) but for situations (a)/(b) without a large scale cloud scheme, and (c)/(d) without a deep convection scheme in the TL/AD model.

#### 4. Summary

The sensitivity analysis system for the T-PARC project was developed by JMA using the SV method to provide guidance for special observations, thereby contributing to improvement of the analysis/forecast field by data assimilation. In addition to three fixed target areas with a 48-hour OTI, which were common among the SV providers, JMA conducted further sensitivity analysis for an adaptive target area with a 24-hour OTI in the vicinity of a TC. The location of the adaptive target area was automatically decided by the operational GSM. We applied a moist SV with a moist TE norm, and both a deep convection and a large-scale cloud scheme were implemented in the TL/AD model. This system worked well, and the related daily products were compared on the website during the T-PARC period.

The case study of daily sensitivity guidance for typhoon Sinlaku highlighted a number of features. In the recurvature stage, due to the longer OTI and the higher latitude target areas, SVs with fixed target areas tended to capture the remote influence of the mid-latitude trough compared to the SV for the adaptive target area. The adaptive target area with a 24-hour OTI therefore seems preferable for the detection of sensitive areas in the TC's vicinity. The nonlinear evolved perturbation from the initial SV shows a structure similar to that of the linearly evolved final SV,

indicating the legitimacy of the linearity assumption in calculating the SV. The results also suggest that moisture convergence and deep convection caused heat release and associated vorticity to the east of Sinlaku at the confluence between the typhoon itself and the subtropical high-pressure system.

On the other hand, some extra experiments were conducted using JMA's sensitivity analysis system to investigate the influence of different configurations among SV providers in the T-PARC project. Without a water vapor effect in the norm, the sensitive areas in the eastern confluence location and the upstream mid-latitude trough become relatively weak. These trends stood out in the dry SV, having no convection and a large-scale cloud scheme, with a dry TE norm. Further experiments revealed that the convection scheme in the TL/AD model played an important role in forming the characteristics of the SV, which followed the mechanism of moisture convergence and associated convection in the eastern confluence location.

Future experiments should focus on building a comprehensive understanding of JMA's SV characteristics through statistical investigation, which will contribute to the development of a new JMA operational global analysis system as well as TEPS and WEPS.

## References

- Aberson, S. D., 2003: Targeted observations to improve operational tropical cyclone track forecast guidance. *Mon. Wea. Rev.*, **131**, 1613-1628.
- Bessho, K., T. Nakazawa, and M. Weissmann, 2010: Dropsonde operation of FALCON in T-PARC and the analysis of surrounding environment of typhoons. *RSMC Tokyo-Typhoon Center Technical Review*, **12**, in press.
- Barkmeijer, J., R. Buizza, T. N. Palmer, K. Puri, and J.-F. Mahfouf, 2001: Tropical singular vectors computed with linearized diabatic physics. *Quart. J. Roy. Meteor. Soc.*, **127**, 685-708.
- Buizza, R., 1994: Sensitivity of optimal unstable structures. *Quart. J. Roy. Meteor. Soc.*, **120**, 429-451.
- Chen, J.-H., M. S. Peng, C. A. Reynolds, and C.-C. Wu, 2009: Interpretation of tropical cyclone forecast sensitivity from the singular vector perspective. *J. Atmos. Sci.*, **66**, 3383-3400.
- Coutinho, M. M., B. J. Hoskins, R. Buizza, 2004: The influence of physical processes on extratropical singular vectors. *J. Atmos. Sci.*, **61**, 195-209.
- Elsberry, R. L., and P. A. Harr 2008: Tropical cyclone structure (TCS-08) field experiment science basis, observational platforms, and strategy. *Asia-Pacific J. Atmos. Sci.*, **44**, 209-231.
- Hoskins, B. J. and M. M. Coutinho, 2005: Moist singular vectors and the predictability of some high impact European cyclones. *Quart. J. Roy. Meteor. Soc.*, **131**, 581-601.
- Kim, H. M., and B.-J. Jung, 2009: Singular vector structure and evolution of a recurring tropical cyclone. *Mon. Wea. Rev.*, **137**, 505-524.
- Kim, H. M., B.-J. Jung, S.-M. Kim, 2010: Real-time adaptive observation guidance of Yonsei University for THORPEX-PARC. in preparation.
- Komori, T., R. Sakai, H. Yonehara, K. Sato, T. Miyoshi, M. Yamaguchi and T. Nakazawa, 2009: JMA's Total Energy Singular Vector Sensitivity Guidance for Adaptive Observations during T-PARC

2008. *CAS/JSC WGNE Research Activities in Atmospheric and Oceanic Modeling*, **39**. Available online at [http://www.wmo.int/pages/about/sec/rescrosscut/resdept\\_wgne.html](http://www.wmo.int/pages/about/sec/rescrosscut/resdept_wgne.html) (WGNE Blue Book)
- Komori, T. and T. Kadowaki, 2010: Resolution Dependence of Singular Vectors Computed for Typhoon SINLAKU. *SOLA*, **6**, 045-048.
- Langland, R. H., 2005: Issues in targeted observing. *Quart. J. Roy. Meteor. Soc.*, **131**, 3409-3425.
- Lorenz, E. N., 1955: Available potential energy and the maintenance of the general circulation. *Tellus*, **7**, 157-167.
- Majumdar, S.J., S. D. Aberson, C. H. Bishop, R. Buizza, M. S. Peng, and C.A. Reynolds, 2006: A comparison of adaptive observing guidance for Atlantic tropical cyclones. *Mon. Wea. Rev.*, **134**, 2354-2372.
- Peng, M. S., and C. A. Reynolds, 2006: Sensitivity of tropical cyclone forecasts as revealed by singular vectors. *J. Atmos. Sci.*, **63**, 2308-2328.
- Reynolds, C. A. and Rosmond, T. E., 2003: Nonlinear growth of singular-vector-based perturbations. *Quart. J. Roy. Meteor. Soc.*, **129**, 3059-3078.
- Reynolds, C. A., M. S. Peng, S. J. Majumdar, S. D. Aberson, C. H. Bishop, and R. Buizza, 2007: Interpretation of adaptive observing guidance for Atlantic tropical cyclones. *Mon. Wea. Rev.*, **135**, 4006-4029.
- Reynolds, C. A., M. S. Peng, and J.-H. Chen, 2009a: Recurring Tropical Cyclones: Singular Vector Sensitivity and Downstream Impacts. *Mon. Wea. Rev.*, **137**, 1320-1337.
- Reynolds, C. A., J. D. Doyle, R. M. Hodur, and H. Jin, 2009b: Naval Research Laboratory Multi-scale Targeting Guidance for T-PARC and TCS-08. *Weather and Forecasting*, in press.
- Sakai, R., M. Kyouda, M. Yamaguchi, and T. Kadowaki, 2008: A new operational one-week Ensemble Prediction System at Japan Meteorological Agency. *CAS/JSC WGNE Research Activities in Atmospheric and Oceanic Modelling*, **38**. Available online at [http://www.wmo.int/pages/about/sec/rescrosscut/resdept\\_wgne.html](http://www.wmo.int/pages/about/sec/rescrosscut/resdept_wgne.html) (WGNE Blue Book)
- Wu, C.-C., J.-H. Chen, P.-H. Lin, and K.-H. Chou, 2007: Targeted observations of tropical cyclone movement based on the adjoint-derived sensitivity steering vector. *J. Atmos. Sci.*, **64**, 2611-2626.
- Wu, C.-C., J.-H. Chen, S.-G. Chen, S. J. Majumdar, M. S. Peng, C. A. Reynolds, S. D. Aberson, R. Buizza, M. Yamaguchi, T. Nakazawa, and K.-H. Chou, 2009: Intercomparison of targeted observation guidance for tropical cyclones in the western North Pacific. *Mon. Wea. Rev.*, **137**, 2471-2492.
- Yamaguchi, M. and T. Komori, 2009: Outline of the Typhoon Ensemble Prediction System at the Japan Meteorological Agency. *RSMC Tokyo-Typhoon Center Technical Review*, **11**, 14-24. Available online at <http://www.jma.go.jp/jma/jma-eng/jma-center/rsmc-hp-pub-eg/techrev.htm>
- Yamaguchi, M., R. Sakai, M. Kyoda, T. Komori, and T. Kadowaki, 2009: Typhoon Ensemble Prediction System Developed at the Japan Meteorological Agency. *Mon. Wea. Rev.*, **137**, 2592-2604.
- Yamashita, K., Y. Ohta and T. Nakazawa, 2009: An Observing System Experiment on the Special Observations of T-PARC for Typhoons Sinlaku and Jangmi using the Operational NWP System at JMA. *CAS/JSC WGNE Research Activities in Atmospheric and Oceanic Modelling*, **39**. Available online at [http://www.wmo.int/pages/about/sec/rescrosscut/resdept\\_wgne.html](http://www.wmo.int/pages/about/sec/rescrosscut/resdept_wgne.html) (WGNE Blue Book)

Yamashita, K. and Y. Ohta, 2010: Observing system experiments using the operational NWP system of JMA. *RSMC Tokyo-Typhoon Center Technical Review*, **12**, in press.



# **Observing-system Experiments Using the Operational NWP System of JMA**

**Koji Yamashita**

Numerical Prediction Division, Japan Meteorological Agency, Tokyo, Japan

**Yoichiro Ohta**

Numerical Prediction Division, Japan Meteorological Agency, Tokyo, Japan

**Kiyotomi Sato**

Numerical Prediction Division, Japan Meteorological Agency, Tokyo, Japan

**Tetsuo Nakazawa**

Meteorological Research Institute, Japan Meteorological Agency, Tsukuba, Japan

## **Abstract**

The Numerical Prediction Division of the Japan Meteorological Agency (JMA) conducted observing-system experiments (OSEs) using the operational NWP system of JMA targeted for typhoons Sinlaku (0813) and Jangmi (0815) with T-PARC special observations in 2008. In many cases, positive impacts were found both in track and intensity forecasts using these observations. Additionally, assimilation of operational tropical cyclone (TC) bogus data contributed to the improvement of track and intensity forecasts at the before-recurvature stage, although it degraded track forecasts in some cases. Investigating the usage of special observations in the operational system revealed a number of problems with the assimilation of horizontally dense dropwindsonde observations. In verification of the sensitivity analysis system, OSEs using T-PARC special observations over a high-sensitivity area showed better performance in TC track forecasts for Sinlaku. These results are expected to contribute to improving the TC forecasts of the NWP system in the near future.

## **1. Introduction**

Under the cooperation of the North American, Asian and European THORPEX Regional Committees, the THORPEX Pacific Asian Regional Campaign (T-PARC) for typhoon track forecasts in the summer of 2008 was run, and included special observation techniques such as dropwindsondes from aircraft, extra upper soundings by JMA observatories and research-vessel monitoring. In addition, Meteorological Satellite Center of JMA (MSC) produced MTSAT-2 Rapid Scan Atmospheric

Motion Vectors for T-PARC (MTSAT-2-RS-AMV). OSEs using the operational NWP system of JMA were performed for typhoons Sinlaku and Jangmi with T-PARC special observations. The aim of the OSEs was to demonstrate the impact of special observations and the effectiveness of the next-generation Interactive Forecast System.

This paper describes the OSE results. Sections 4.2 and 4.3 give a brief outline of the global NWP system and the experimental design. Section 4.4 gives the OSE results and details some case studies. Section 4.5 summarizes the results and concludes the paper.

## 2. Outline of the global NWP system

All experiments were conducted using the operational JMA GSM (TL959L60, horizontal resolution approx. 20 km) and 4D-Var data assimilation system (inner resolution T159L60, horizontal resolution approx. 80 km, 6-hour assimilation window). An outline of the global NWP system is given in Table 1. More details of the system can be found in Nakagawa (2009).

Table 1 Outline of the global NWP system at JMA

| Global Data Assimilation System |  |
|---------------------------------|--|
| Method                          | 4D-Var   |
| Resolution (inner model)        | T159L60 (Gaussian grid, horizontal resolution approx. 80 km, model top 0.1 hPa)    |
| Assimilation window             | 6 hours ( $\pm 3$ hours, time slots approx. 1 hour)                                |
| TC bogus data                   | Not used in TEST and CNTL experiments but assimilated in operational run and BOGUS |

| Global Spectral Model |  |
|-----------------------|--|
| Resolution            | TL959L60 (reduced Gaussian grid, horizontal resolution approx. 20 km, model top 0.1 hPa) |
| Forecast time         | 84 hours/216 hours (00, 06, 18 UTC/12 UTC)   |

## 3. Experimental design

Three experiments were performed in T-PARC:

- (I) Special observations were assimilated with techniques including dropwindsonde from aircraft, upper soundings from JMA observatories and research-vessel monitoring (TEST).
- (II) TC bogus data (JMA 2007) were assimilated instead of special observations (BOGUS).
- (III) No special observations or bogus data were assimilated (CNTL).

The aims of BOGUS were to evaluate the current TC bogus technique and investigate the relative importance of special observations in an operational context.

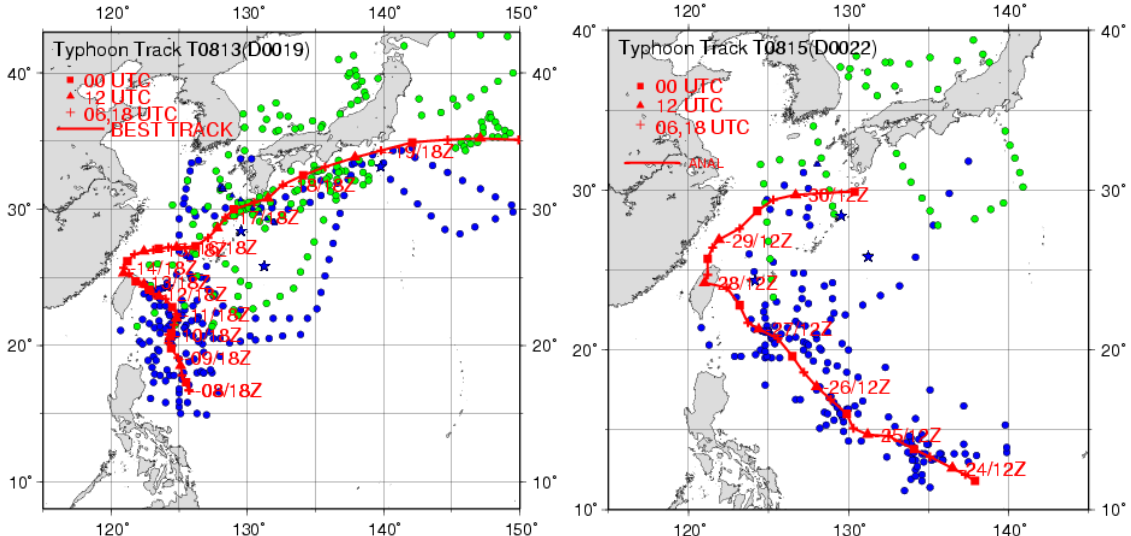


Figure 1 The observed tracks of Sinlaku (left) and Jangmi (right) and the positions of special observations. The blue and green plots show special observations at the before- and after-recurvature stages, respectively. The red solid lines show the best tracks of Sinlaku and Jangmi.

The experimental periods were from 00 UTC on 9 September 2008 (0900; hereafter the date and time are abbreviated as *ddhh* without the month) to 1818 for Sinlaku and from 2412 to 3018 for Jangmi. The observed tracks of the two typhoons are shown in Figure 1. Hereafter, the period is divided into two stages. One is the before-recurvature stage (Sinlaku: before 1418; Jangmi: before 2818), and the other is the after-recurvature stage (Sinlaku: after 1500; Jangmi: after 2900). The effect of the special observations and TC bogus data remained in the later analysis through the data assimilation cycle. For the case study, the first guess was taken from the CNTL run; 84-hour forecasts for all initial times and 216-hour forecasts for the selected cases were conducted. TC track forecasts were verified using the TC best track provided by the RSMC Tokyo - Typhoon Center (OBS). The results of the OSEs were evaluated with CNTL.

#### 4. OSE results

##### 4.1 Sinlaku (0813)

###### (a) Track forecasts

In the before-recurvature stage from 0900 to 1418, the TC track errors of TEST were reduced compared to CNTL by between 23 and 30% for first-12-hour forecasts, and by approximately 10% for 18- to 48-hour forecasts. The results for the first-12-hour forecasts are statistically significant with a 95% confidence level (hereafter referred to simply as statistically significant). The TC track errors of BOGUS increased by between 10 and 23% for first-30-hour forecasts, although the TC track position for BOGUS was close to OBS at the initial time. On the other hand, for 60- to 72-hour forecasts, the track errors were reduced by approximately 15% (Figure 2).

In the after-recurvature stage from 1500 to 1818, the TC track errors of TEST showed a statistically significant reduction of about 10% for 66- to 84-hour forecasts. However, the TC track errors of BOGUS remained almost the same as those of CNTL (Figure 3). These results are not

statistically significant. A forecast initialized at 0912 is shown in Figure 4. The tracks of both TEST and BOGUS are closer to OBS data than those of CNTL.

(b) Intensity forecasts

The intensity forecasts were evaluated using the mean errors of the central pressure forecasts. Figure 5 shows the results for the before-recurvature stage of Sinlaku. In this case, intensity forecast errors showed a statistically significant reduction over 10 hPa in both TEST for 36-hour forecasts and BOGUS for 24-hour forecasts. On the other hand, the impact on the intensity forecasts in TEST was almost neutral in the after-recurvature stage. In the case of BOGUS, however, the intensity forecasts showed negative pressure errors after the 12-hour stages (Figure 6). Since the typhoon was not in the extra-tropical transition stage in this case, one reason may be that the operational NWP model did not create a realistic typhoon structure.

(c) Impact of special observations on TC track predictions at 1112

Figure 7 shows the TC track forecasts of TEST, BOGUS and CNTL at 1112. BOGUS and CNTL followed a track close to that of OBS at the beginning. The TC track forecasts of TEST showed rapid recurvature, and this fast movement resulted in large track errors. We found that dropwindsonde observations in the TC core fields within 200 km were assimilated (Figure 8). The positions of observed wind circulations on each vertical level were different from those of OBS, bringing a biased and warped vortex to the south in the analysis. The analysis fields for comparison of TEST with CNTL are shown in Figure 9 as the differences between these results. Deepened geopotential height and strengthened vortex circulation to the south and east of the TC center are found. The TC generally tends to be moved to a deeper geopotential height, and moved southward then northeastward. It can therefore be said that dropwindsonde data for the core region of the TC have a large impact on TC forecasts. However, quality control (QC) procedures for observational data around the TC center are difficult. This problem requires further investigation in the future.

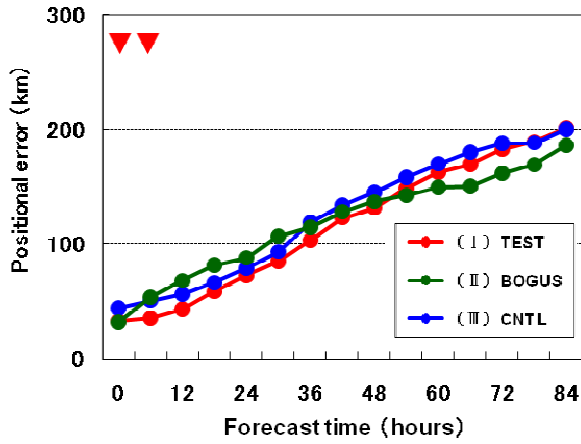


Figure 2 Positional errors for Typhoon Sinlaku in the before-recurvature stage from 0900 to 1418. The red line is for TEST, which assimilated special observations. The blue line is for CNTL, which did not assimilate special observations. The green line is for BOGUS, which assimilated TC bogus data but did not use special observations. The red triangles denote that the difference of TEST minus CNTL is statistically significant with a 95% confidence level.

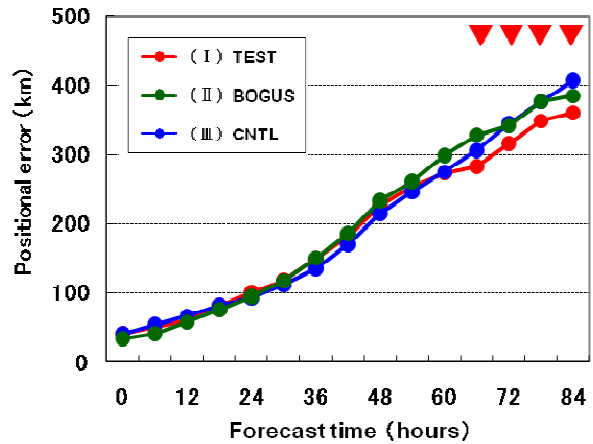


Figure 3 As per Figure 2, but for the after-recurvature stage

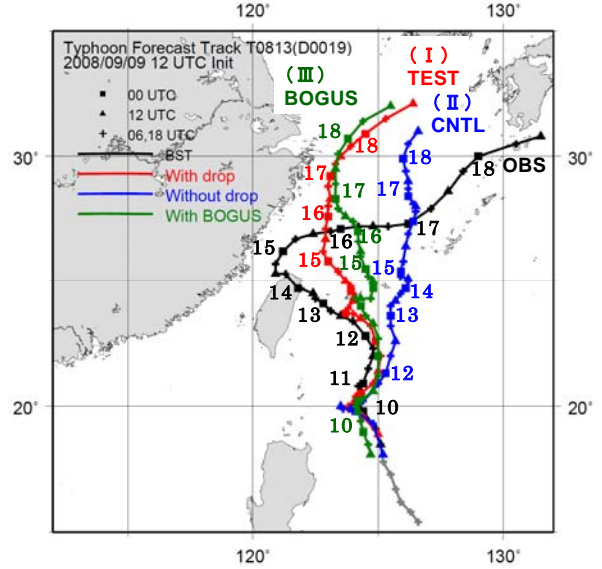


Figure 4 Typhoon track forecasts from the OSEs with (red markers: TEST) and without (blue markers: CNTL) special observations and with BOGUS data (green markers) for Typhoon Sinlaku, initialized at 0912. The black markers show OBS data. The numbers indicate the date of the typhoon's location at 00 UTC.

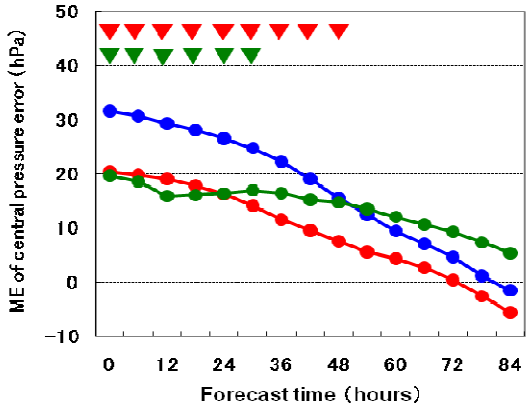


Figure 5 Mean error of TC central pressure forecast for Typhoon Sinlaku in the before-recurvature stage from 0900 to 1418. The line notation is the same as that in Figure 2. The red triangles denote that the result of TEST minus CNTL is statistically significant with a 95% confidence level, and the green triangles denote that the result of BOGUS minus CNTL is statistically significant.

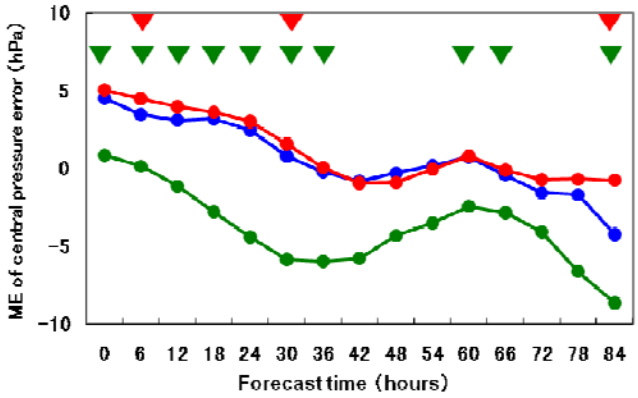


Figure 6 As per Figure 5, but for the after-recurvature stage

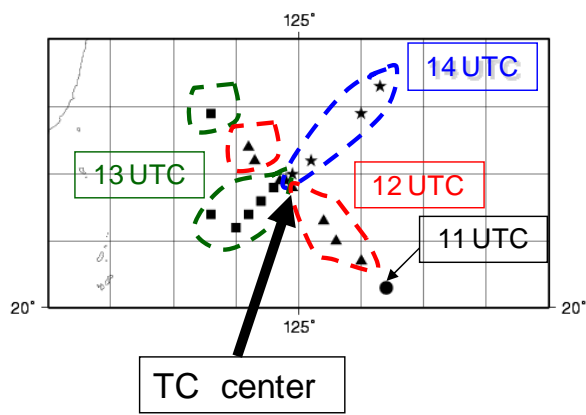


Figure 8 C-130 special observations from 1111 to 1114, initialized at 1112. Black star, triangle, square and circle plots show the positions of C-130 dropwindsonde observations.

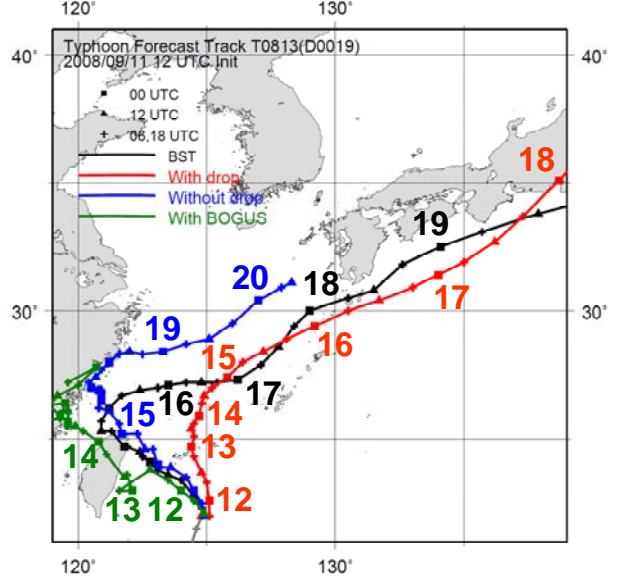


Figure 7 Typhoon track forecasts from the OSEs with (red markers: TEST) and without (blue markers: CNTL) C-130 special observations and with BOGUS data (green markers) for Typhoon Sinlaku, initialized at 1112. The black markers show OBS data. The numbers indicate the date of the typhoon's location at 00 UTC.

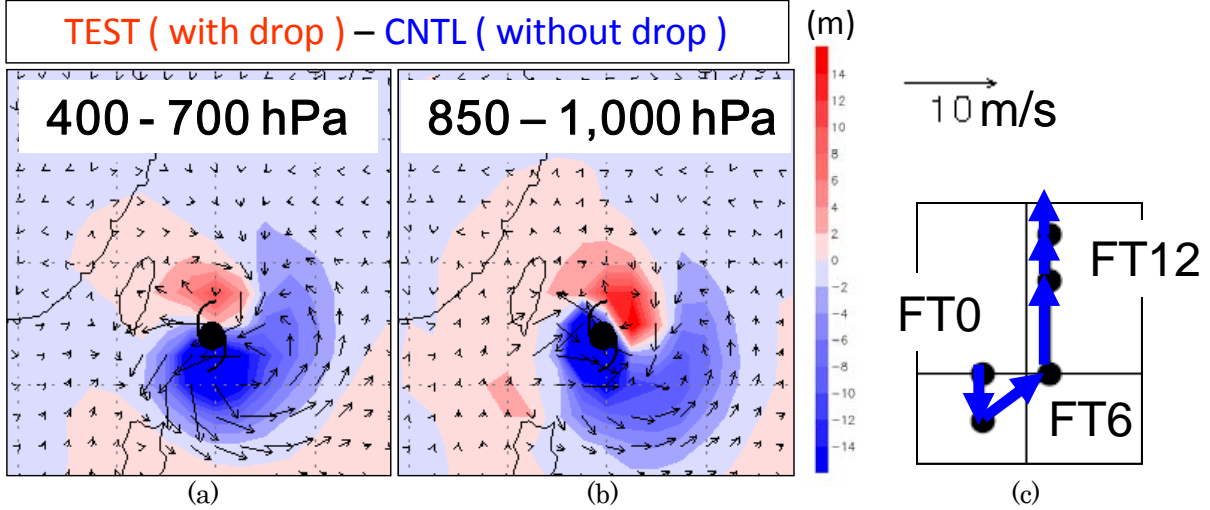


Figure 9 Averaged wind vectors and geopotential height differences ((a) vertically averaged from 400 hPa to 700 hPa; (b) vertically averaged from 850 hPa to 1,000 hPa) defined as TEST minus CNTL in the analysis at 1112. FT represents the forecast time from the initial time. The positions of the typhoon plots and FT0 show the TC center of Typhoon Sinlaku at 1112. (c) TC track forecast of TEST initiated at 1112 from FT0 to FT12.

#### (d) Verification of sensitivity analysis system

To investigate the effectiveness of the sensitivity analysis system, we conducted another OSE for special observations in the first mode of the high sensitivity area calculated using the singular vector (SV) method (Komori et al., 2010). The verification times were 1100 and 1000 for 24-hour forecasts initiated at 1000 and 0900 (Figures 10 and 11). In these cases, two high-sensitivity areas were found to the northeast and southwest of the TC center. Three numerical experiments were carried out with different special observations as follows:

- (I) Special observations to the northeast of the TC center (CASE\_A)
- (II) Special observations to the southwest of the TC center (CASE\_B)
- (III) Both CASE\_A and CASE\_B (CASE\_A+B)
- (IV) No special observations (CNTL)
- (V) CASE\_A without humidity (only OSE for 1100: NOVAPOR)

In the case of 1100, the TC track mean errors of CASE\_A were reduced from those of CNTL by between 32% and 45% for the early stages and by 16% after 60 hours. In this case, special observations in the northeastern high-sensitivity area were more effective in improving the TC track forecast. Improvements for NOVAPOR and CASE\_A+B of between 32% and 45% for the early stages and of 10% after 60 hours were also found (Figure 12). Comparing CASE\_A and NOVAPOR, CASE\_A after the 60-hour forecast point showed a smaller improvement than NOVAPOR, indicating that humidity observations contributed to the improvement of TC track forecasts after 60 hours. On the other hand, the mean track errors in CASE\_B increased, which may be because the observations did not fit the analysis and the number of special observations for CASE\_B was much lower than that

in CASE\_A. However, these are not considered to be the only reasons for the increased track errors in CASE\_B.

In the case of 1000, the TC track errors for CASE\_A increased, although this case had observations in the high-sensitivity area. On the other hand, the TC track errors were reduced in CASE\_B with observations in the low-sensitivity area. The special observations in CASE\_B were reflected appropriately in the analysis both to the southwest and to the northeast of the TC center, resulting in the best forecasts for CASE\_B. As for CASE\_A, correction of counterclockwise circulation to the northeast of the TC center was found in the analysis, causing the typhoon to move northward and resulting in worse TC track forecasts. The impact of CASE\_A+B was almost neutral (Figure 13).

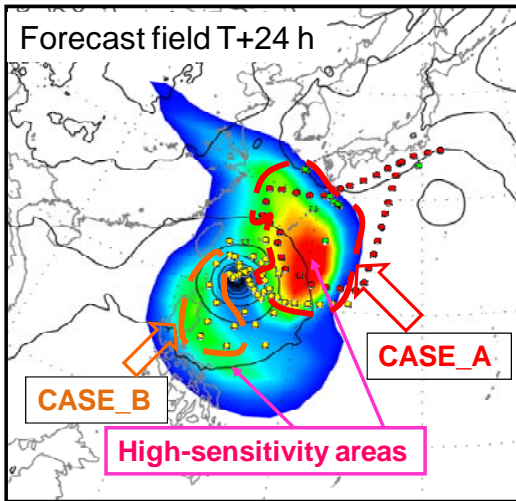


Figure 10 The sensitive areas in the first mode calculated from the one-day forecast field valid for 1100. Extra observation points for upper-soundings by JMA research vessels and ground observatories (green points), dropsondes released by Falcon aircraft (red) and those released by other planes (yellow) are overlaid on the high-sensitivity areas.

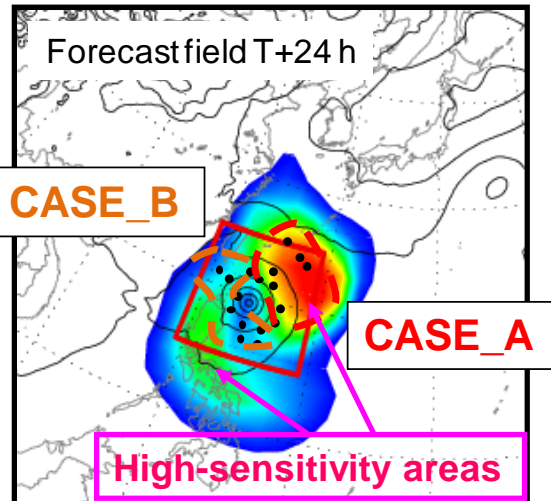


Figure 11 As per Figure 10, but from the one-day forecast field valid for 1000. Observation points for dropsondes released by DOTSTAR aircraft (black) are overlaid on the high-sensitivity areas.

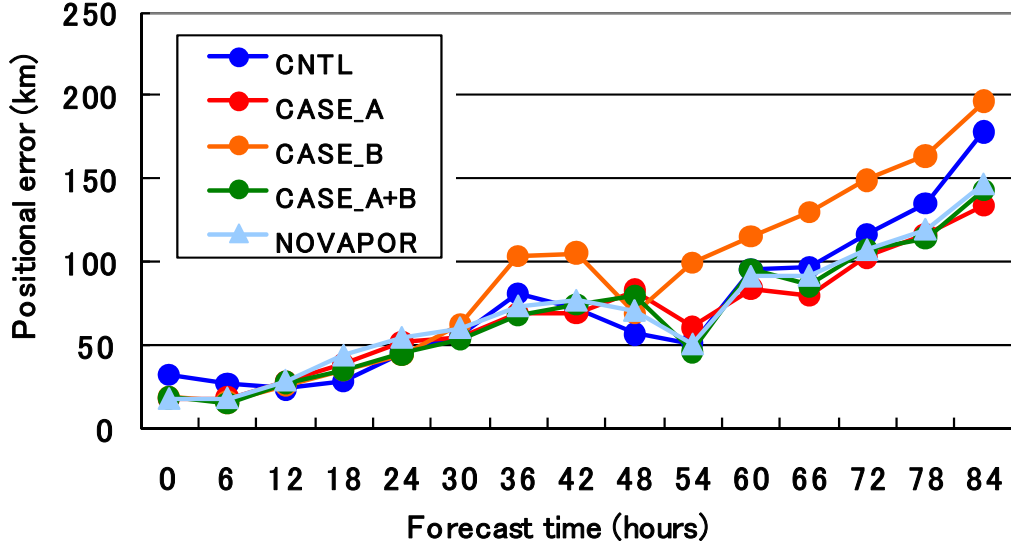


Figure 12 Mean TC track forecast errors of Typhoon Sinlaku for CASE\_A (red lines), CASE\_B (orange), CASE\_A+B (green), NOVAPOR (thin blue) and CNTL (blue) from 1100 to 1112

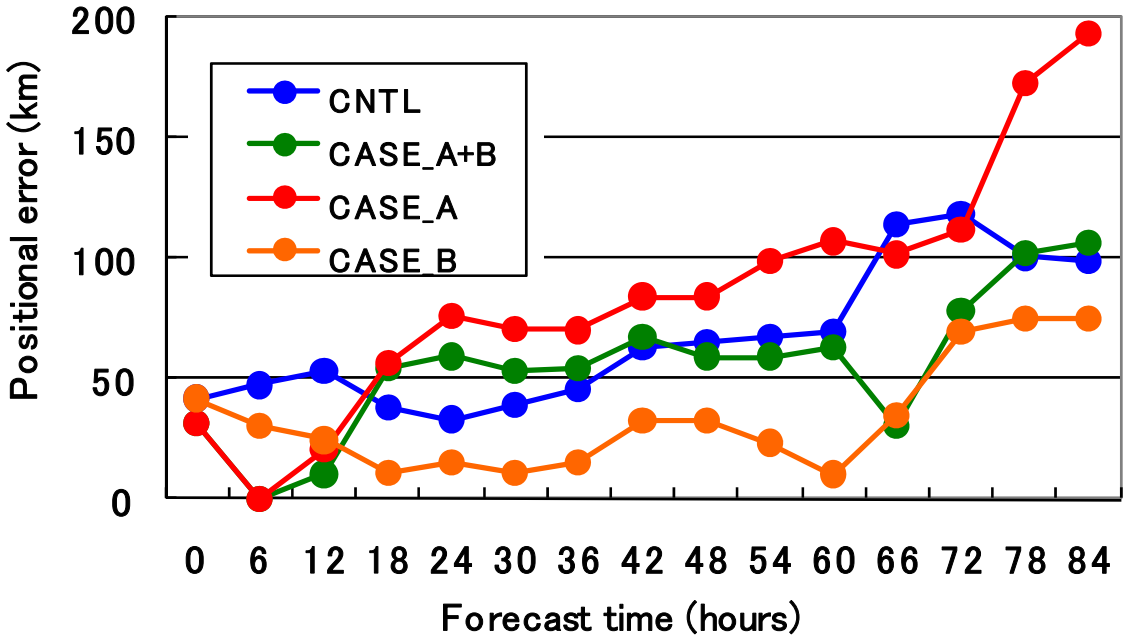


Figure 13 TC track forecast errors of Typhoon Sinlaku for CASE\_A (red lines), CASE\_B (orange), CASE\_A+B (green) and CNTL (blue) at 1000

#### (e) Trial of OSEs using MTSAT-2-RS-AMV

MSC produced MTSAT-2-RS-AMV data derived from three consecutive images with intervals of 15 minutes (MTSAT-2-RS-AMV\_15MIN), 7 minutes (MTSAT-2-RS-AMV\_7MIN) and 4 minutes (MTSAT-2-RS-AMV\_4MIN) for T-PARC. The OSEs for MTSAT-2-RS-AMV were conducted with an initial time of 1718. The NWP system was the same as that of the OSEs for special observations (see Section 4.2). The experimental design is outlined in Table 2.

Table 2 Experimental design of OSEs for MTSAT-2 Rapid Scan AMV

|                         | TEST     | CNTL     |
|-------------------------|----------|----------|
| TC bogus data           | Not used | Not used |
| Special observations    | Not used | Not used |
| MTSAT-2 Rapid Scan AMVs | Used     | Not used |
| Other observations      | Used     | Used     |

In TEST, a two-step thinning scheme was used as a trial. In this method, MTSAT-2-RS-AMV\_4MIN and MTSAT-2-RS-AMV\_7MIN are thinned to a resolution of 100 km (one AMV in each 1 deg. x 1 deg. x 100 hPa box in the hourly time window) after 200-km thinning (one AMV in each 2 deg. x 2 deg. x 100 hPa box in the six-hour time window) of the other AMVs. The other QC is the same as that for other AMVs. More details on the QC of AMVs can be found in JMA (2007) and Yamashita (2008). Figure 14 shows examples of AMVs after QC at 18 – 19 UTC on

17 September 2008.

As a result, the slow bias speeds for TC track forecasts were slightly improved, indicating the possibility of improvement for TC track forecasts using MTSAT-2-RS-AMV data (Figure 15 and Figure 16).

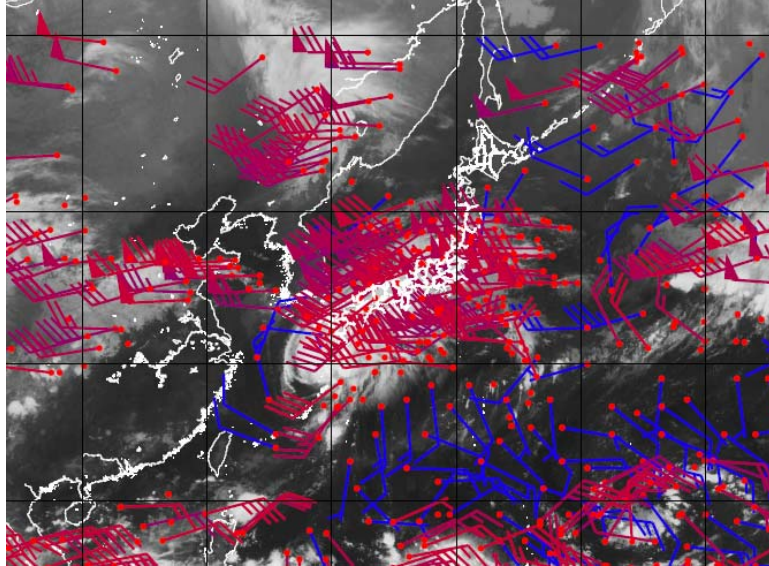


Figure 14 Distribution of MTSAT-2-RS-AMVs after QC from 1718 to 1719. High layer wind barbs (less than 500 hPa, red wind barbs) and low ones (greater than 850 hPa, blue wind barbs) are overlaid on the MTSAT-1R IR image. The unit of wind barbs is knots. Wind half-barbs are 5 knots, and full barbs are 10 knots. Wind flags are 50 knots.

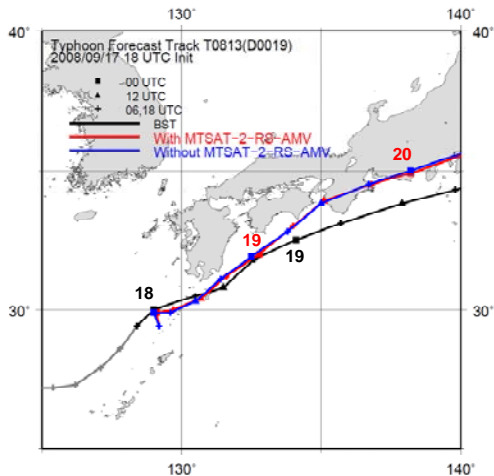


Figure 15 Typhoon track forecasts from OSEs with TEST (red markers) and CNTL (blue markers) for Typhoon Sinlaku with an initial time of 1718. The black markers show OBS data. The numbers indicate the date of the typhoon's location at 00 UTC.

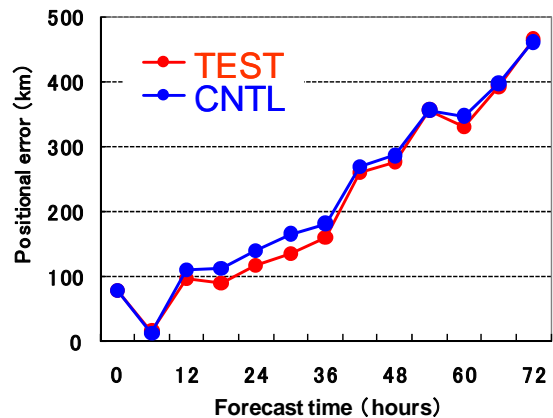


Figure 16 TC track forecast errors of Typhoon Sinlaku for TEST and CNTL with an initial time of 1718

## 4.2 Jangmi (0815)

### (a) Track forecasts

Figure 17 shows average TC track forecast errors for Jangmi in the before-recurvature stage. In this stage, both special observations and TC bogus data improved the track forecasts (24 to 42% with 0- to 18-hour forecasts for TEST and 25% with the 6-hour forecast for BOGUS). It appears that the analysis field was improved using special observations or TC bogus data at the before-recurvature stage because Jangmi was located in an area where conventional observation data were sparse. For BOGUS, the track forecasts became degraded after the 30-hour forecast stage. Figure 18 shows a scatter diagram of positional errors for the 72-hour forecast. With TC bogus data, some forecast tracks were shifted significantly leftward and decelerated. These cases made the average track forecast errors worse.

Figure 19 is the same as Figure 17, but for the after-recurvature stage. No significant difference was found between the mean track forecast errors for TEST and CNTL. As for BOGUS, the track forecasts were slightly degraded for forecasts between 18 to 54 hours and slightly improved for other forecast times.

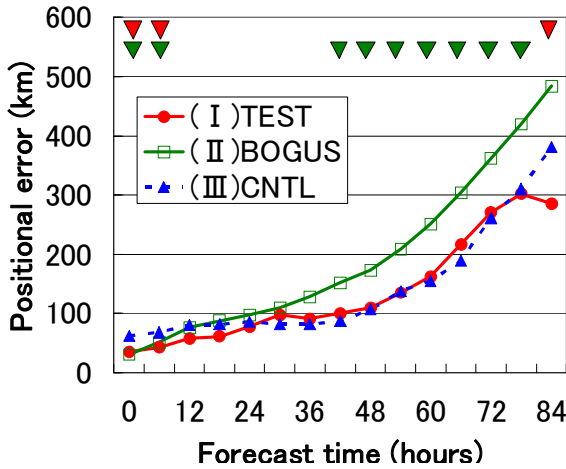


Figure 17 Average TC track forecast errors for Jangmi at the before-recurvature stage. The solid red, solid green and dotted blue lines show the track forecast errors for TEST, BOGUS and CNTL, respectively. The red and green triangles indicate that the differences of error from CNTL are statistically significant at a 95% confidence level.

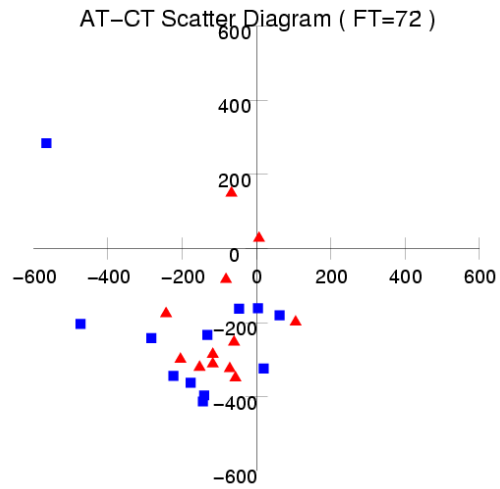


Figure 18 Scatter diagram of TC positional errors for Jangmi in the before-recurvature stage (72-hour forecast). The vertical and horizontal axes denote along-track and cross-track errors. The blue squares and red triangles show BOGUS and CNTL, respectively.

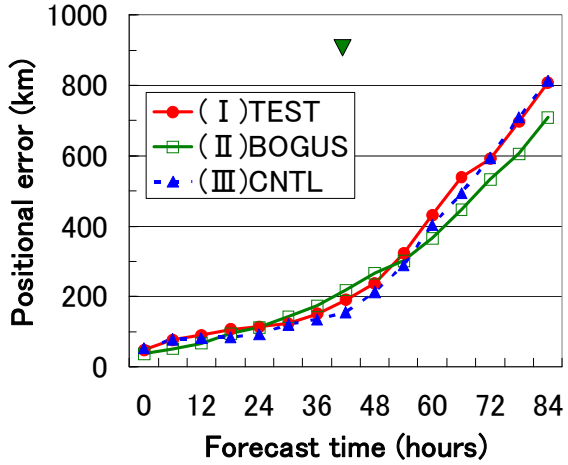


Figure 19 As per Figure 17, but for the after-recurvature stage

#### (b) Intensity forecasts

Figure 20 shows the mean errors of central pressure forecasts at the before-recurvature stage. Without special observations or TC bogus data, the intensity of Jangmi remained too weak considering that it was one of the strongest typhoons of 2008 (the minimum central pressure was 905 hPa). Using special observations or TC bogus data resulted in significant improvements for intensity forecasts, especially the short-range type. It seems that the assimilation of these data made realistic TC structures and helped TC intensification at the development stage.

Figure 21 is the same as Figure 20, but for the after-recurvature stage. No significant difference was found between TEST and CNTL. Using TC bogus data, the intensity forecast showed a TC that was slightly too strong after the 48-hour forecast stage. Since Jangmi was in a period of transition to an extra-tropical cyclone, the forecast after 48-hours appears to have been worse. In this case, using TC bogus data made a cyclone that was too strong after the extra-tropical cyclone transition stage.

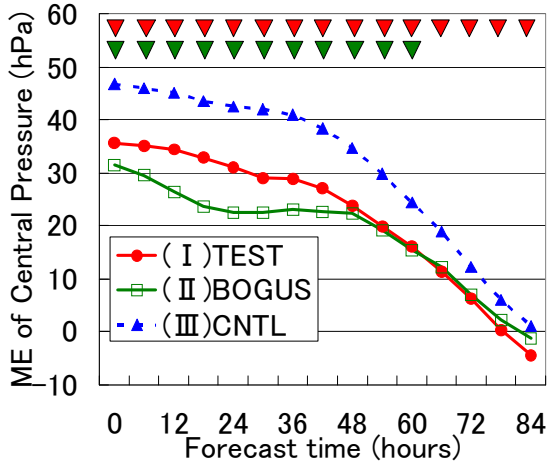


Figure 20 Mean errors of TC central pressure forecast for Jangmi at the before-recurvature stage. The notations of the lines and marks are the same as those in Figure 17.

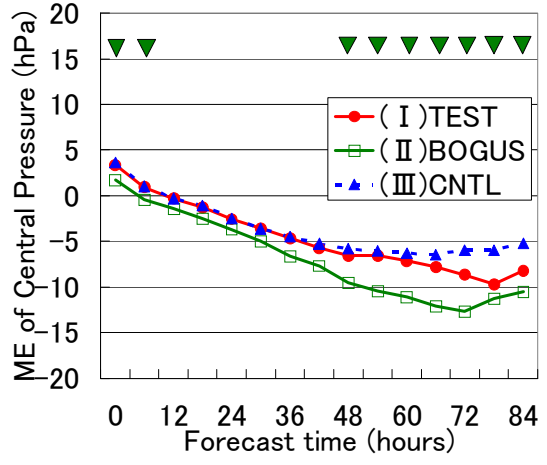


Figure 21 As per Figure 20, but for the after-recurvature stage

### (c) Case study

Further experiments were performed for a number of typical cases. On the forecasts initiated at 2500, the GSM forecast track with special observations showed much better agreement with the observed track and predicted recurvature after landing on Taiwan, which was not the case in the forecast without special observations (Figure 22).

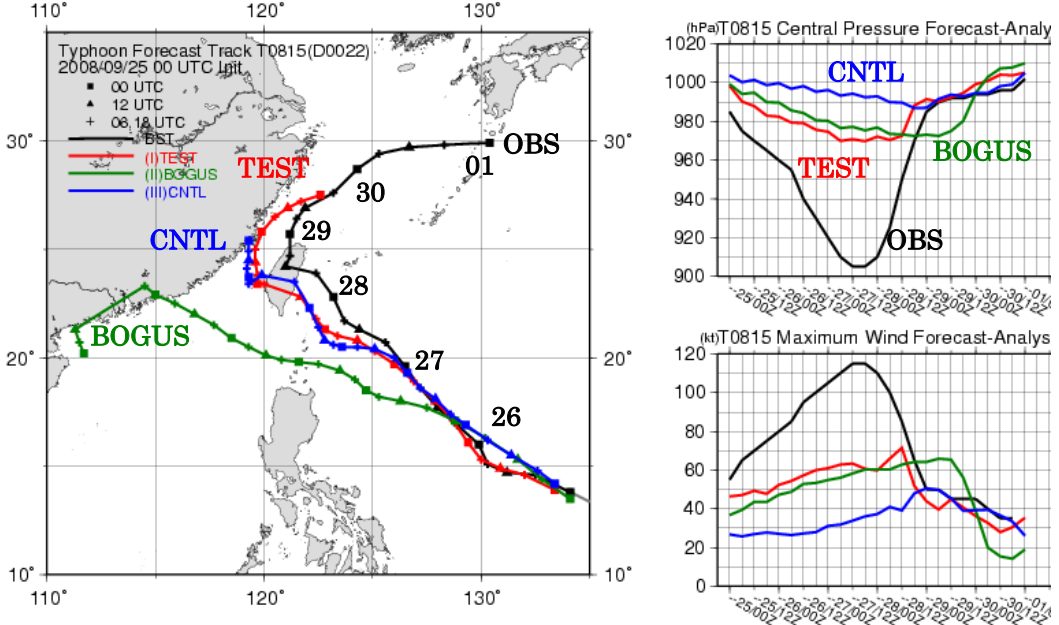


Figure 22 Forecast tracks for Jangmi (initial time 2500). The red, green and blue lines show the forecast tracks of TEST, BOGUS and CNTL, respectively. The black lines show OBS values.

In further experiments, the special observations conducted around this initial time were assimilated separately according to their observation points. Figure 23 shows the forecast without observations (CNTL) and with all observations in the center and the northern quadrant of Jangmi (NC ALL). It was found that using dropwindsonde observations near the center and in the northern quadrant improved the intensity forecast, while using them in the eastern and southern quadrants improved the track forecast (not shown).

An impact study regarding the selection of observation elements was conducted. Each element of dropwindsonde observation (horizontal wind, temperature and humidity) was assimilated separately. In Figure 23, the green lines show the forecast with wind observations to the north and center of Jangmi only (NC WIND). Comparing these forecasts shows that wind observations had the largest impact on the forecast of Jangmi in this case, especially for the short-range track forecast. Other observation elements also had an impact on the intensity forecast.

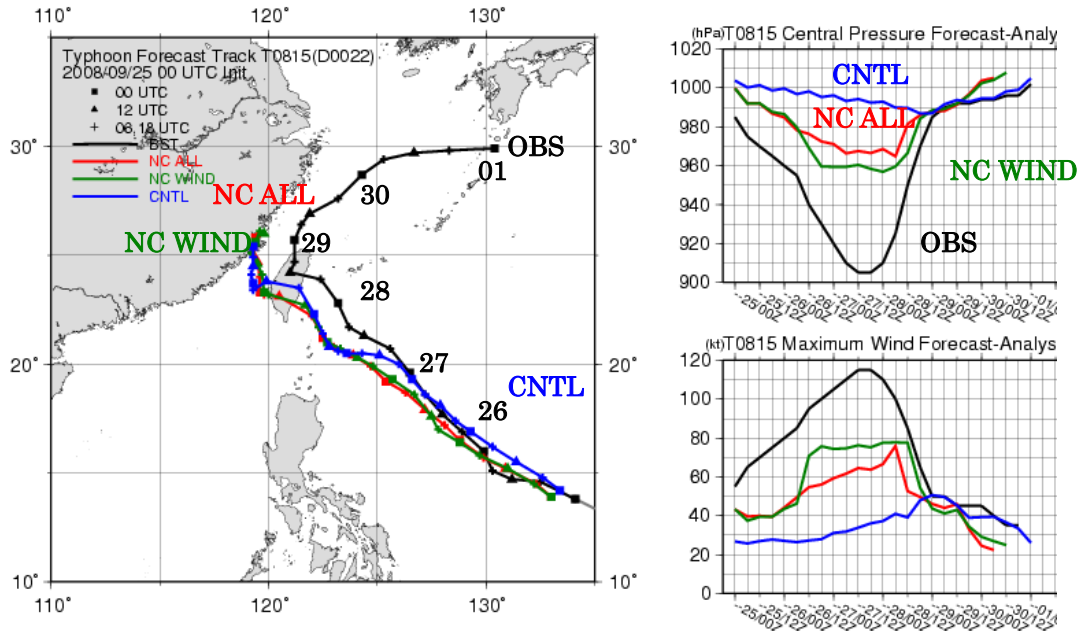


Figure 23 Forecast tracks for Jangmi (initialized at 2500). The red, green and blue lines show the forecast tracks for NC ALL, NC WIND and CNTL, respectively. The black lines show OBS data.

#### (d) Observations and data assimilation system of JMA

The characteristics of the special observations and their usage in the operational global data assimilation system of JMA were investigated. Large differences in wind observations from the first-guess field were found around the center of Jangmi, and these decreased considerably after the analysis. As for the dropwindsonde and additional upper sounding observations, most of those on mandatory levels were assimilated, and no horizontal data thinning was applied. Thus, in most cases, assimilation of these observations contributed to improvement of the analysis field, but there may be some problems with a lack of horizontal thinning for such spatially dense observations. In fact, as mentioned earlier, the assimilation of dropwindsonde observations near the center caused significant degradation of the track forecast in some cases.

## 5. Summary and conclusion

The OSEs performed revealed the positive impacts of special observations in the operational JMA GSM mainly at the before-recurvature stage of Sinlaku and Jangmi. Using TC bogus data also contributed to the improvement of intensity forecasts and short-range track forecasts at the before-recurvature stage. However, the assimilation of TC bogus data sometimes led to a degradation of track forecasts.

Further experiments for Jangmi on a number of typical cases were conducted, and the impact of each observation was investigated. Through these experiments, it was found that wind observation had a large impact on the analysis and forecast fields.

Although the OSEs for Sinlaku and Jangmi demonstrated the effectiveness of special observations, some problems were found with the assimilation of dropwindsonde data, especially for those near the TC centers. These problems need to be investigated in more detail and treated carefully to achieve further TC forecast improvements.

In the verification of the sensitivity analysis system, special observations in high-sensitivity areas were more effective in improving TC track forecasts, indicating the high possibility of their use as interactive forecast system tools. However, as there was a case in which special observations caused deterioration in TC track forecasting, these studies should be continuously implemented to address the problem.

In the trial involving OSEs using MTSAT-2-RS-AMV, the possibility of improvement for TC track forecasts was shown.

## References

- JMA, 2007: Outline of the Operational Numerical Weather Prediction at the Japan Meteorological Agency, March 2007, 17.
- Komori, T., R. Sakai, H. Yonehara, T. Kadokawa, K. Sato, T. Miyoshi and M. Yamaguchi, 2010: Total Energy Singular Vector Guidance developed at JMA for T-PARC. *RSMC Tokyo-Typhoon Center Technical Review*, **12**, in press.
- Nakagawa, M., 2009: Outline of the High Resolution Global Model at the Japan Meteorological Agency. *RSMC Tokyo-Typhoon Center Technical Review*, **11**, 1 – 13.
- Yamashita, K., 2008: Upgraded Usage of Atmospheric Motion Vectors from All Geostationary Satellites in the Operational Global And Meso-Scale 4D-Var Assimilation System at JMA, *Proceedings of 9th IWW*, USA.

## T-PARC Website at MRI

Shunsuke Hoshino and Tetsuo Nakazawa

Meteorological Research Institute, Japan Meteorological Agency

### 1. Overview

The special experiments conducted during the T-PARC project of 2008 produced a great deal of observation and forecast data. For researchers' convenience, a number of related products from the Japan Meteorological Agency (JMA) and other organizations are archived on the T-PARC website at <http://tparc.mri-jma.go.jp/> (Fig. 1). This paper gives a brief introduction to the website's content.

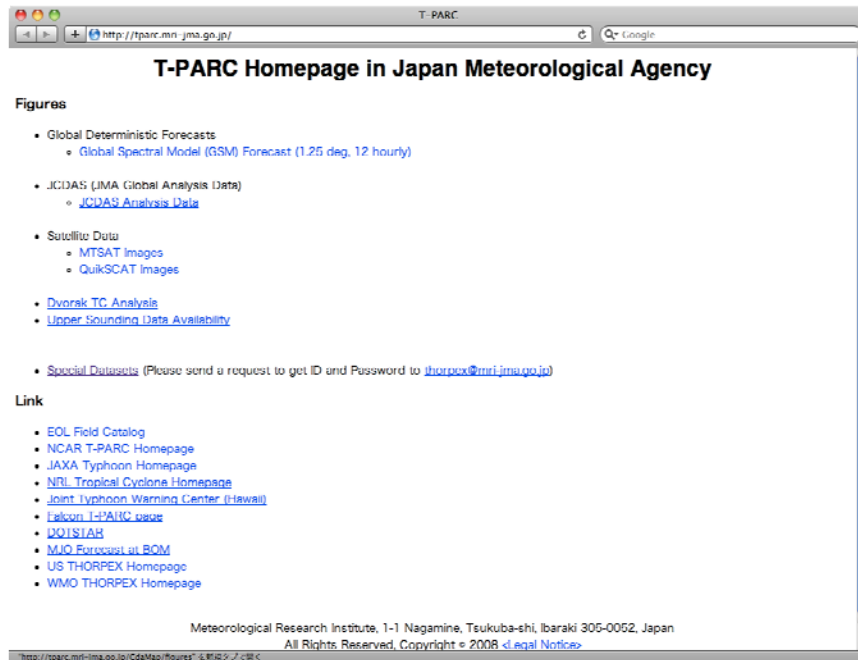


Figure 1 T-PARC website

The T-PARC website operated by the MRI contains both freely available and restricted-access data/products. In this paper, Section 2 details the freely available content, and Section 3 outlines the restricted-access content.

## 2. Freely available content

### 2.1 Global deterministic forecasts

The pictures in PNG format from GSM deterministic forecasts (run twice a day) are provided. The file names and corresponding elements are shown in Table 1. The forecast times are from the initial time to 72 hours ahead at 12-hour intervals. A sample picture is shown in Fig. 2.

| File name | Elements                           |
|-----------|------------------------------------|
| Ps89      | Sea surface pressure [hPa]         |
| Tmp89     | Temperature [K]                    |
| Deprxx    | T-Td [K]                           |
| HTTTdxx   | Height [m], T [K], T-Td [K]        |
| UVxx      | Wind                               |
| Vorxx     | Vorticity [ $10^{-5}$ /s]          |
| Divxx     | Divergence [ $10^{-5}$ /s]         |
| EPV32     | 320K EPV [PVU], P [hPa], wind      |
| 2PVU      | Theta [K], Ps [hPa], wind at 2 PVU |

Table 1 File names of visual representations and corresponding elements. The ‘xx’ parts represent two-digit heights in hPa, and ‘89’ is used for surface data.

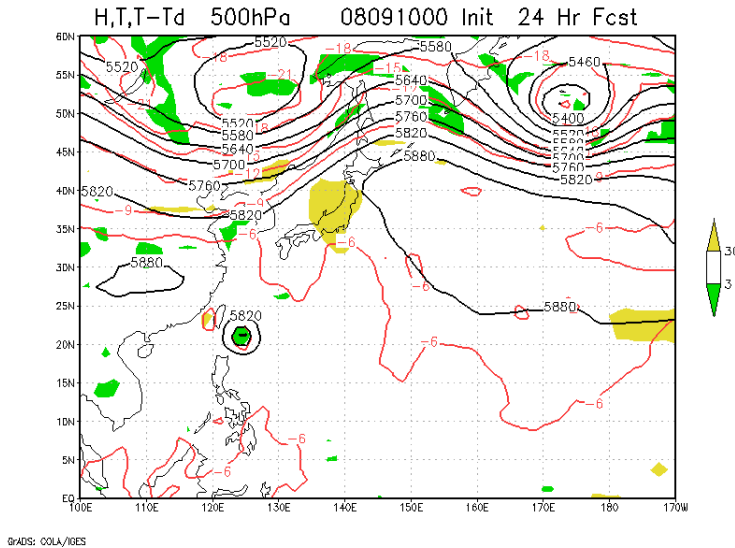


Figure 2 Sample picture of a GSM deterministic forecast

Directories are prepared for each initial time in each month’s directory. Binary data are provided as restricted-access content.

## 2.2 JMA global analysis data (JCDAS)

The pictures of six-hourly JCDAS global analysis data are provided. The elements included are the same as those of GSM deterministic forecasts. Directories are prepared for each date in each month's directory. Binary data are provided as restricted-access content.

## 2.3 Satellite data

Half-hourly MTSAT-1R images from four channels (IR1 (i1), water vapor (wv), VIS (vs) and short-wave IR (i4)) are provided in PNG format covering 100°E – 170°W and EQ – 60°N.

Visual representations of QuikSCAT wind distribution are also provided. These QuikSCAT data are originally provided by Remote Sensing Systems (<http://ssmi.com/>). The representations for descending (ascending) passes are treated as observed at 09 UTC (21 UTC).

For both types of satellite data, directories are prepared for each month. Binary data are provided as restricted-access content.

## 2.4 Dvorak TC analysis

The results of six-hourly Dvorak TC analysis are overlaid on MTSAT-1R IR1 images (Fig. 3). Directories are prepared for each month.

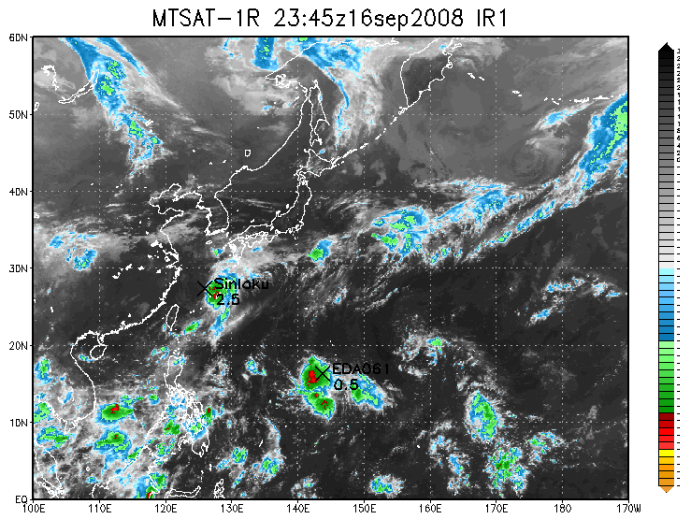


Figure 3 Dvorak TC analysis overlaid on an MTSAT-1R IR1 image

## 2.5 Map of upper-sounding availability

Maps plotting upper-sounding observation stations and global analysis from three hours before to three hours after each analysis time are provided.

### 3. Restricted-access content (for special users)

Restricted-access content is provided from the Special Datasets page at <http://tparc.mri-jma.go.jp/special/special.html> (Fig. 4), accessible from the homepage of the T-PARC website. A user ID and password provided by the administrator ([thorpex@mri-jma.go.jp](mailto:thorpex@mri-jma.go.jp)) are required to access the data.

The resource provides binary data from JCDAS global analysis, GSM forecasts, MTSAT-1R data, QuikSCAT data, JMA in-situ data, pictures and binary data from weekly, monthly and tropical cyclone ensemble forecasts and cyclone XML data. Most of the binary information except for JMA in-situ data can be read with GrADS. Control files to read the GrADS data are also provided.

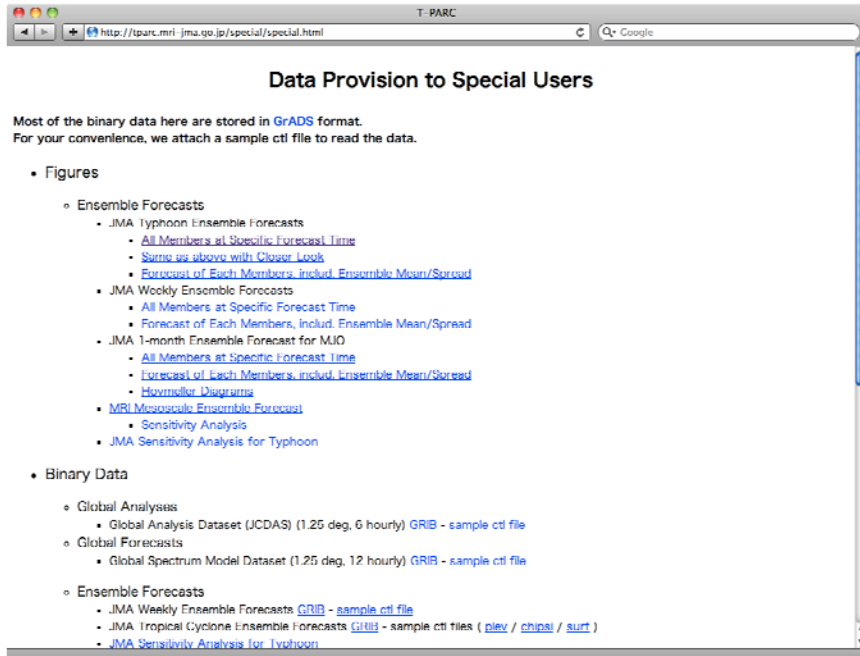


Figure 4 Top page of restricted-access content

#### 3.1 Global analysis data

Six-hourly JCDAS global analysis data are provided in GRIB format with GrADS control files and GRIB index files. These are 1.25-degree-grid data outlining geopotential height, air temperature, specific humidity, dew point depression, zonal wind, meridional wind, cloud water content, and pressure reduced to MSL. Directories are prepared for each date in each month's directory.

### 3.2 Global forecast data

Twelve-hourly GSM deterministic forecast data are provided in GRIB format with GrADS control files and GRIB index files. GSM forecasts cover 1.25-degree grids and include surface total precipitation, mean sea level pressure, geopotential height, dew point depression, temperature, zonal wind, meridional wind and velocity potential. Directories are prepared for each month.

### 3.3 JMA ensemble forecast data

#### 3.3.1 Weekly ensemble forecasts

The GSM weekly ensemble forecasts by day (with an initial time of 12 UTC for each day) are provided in visual and binary format. There are two kinds of pictures: those including all members at a specific forecast time (Fig. 5) and the time-series for each member with the ensemble mean and spread (Fig. 6).

Binary data are provided in gzip compressed format, and consist of GRIB data with GrADS control files and GRIB index files for each initial time. There are three data files for each member: the *plev* file contains, mean sea level pressure, geopotential height, temperature, relative humidity, u wind, v wind and pressure vertical velocity (omg) profiles; the *chpsi* file contains stream function (psi) and velocity potential (chi); and the *surf* file contains surface total precipitation, cloud cover, pressure reduced to MSL, relative humidity 2 m above ground level, temperature 2 m above ground level, and u and v winds 10 m above ground level. Pictures are provided in individual month/initial time directories for each kind, and binary data are provided in monthly directories.

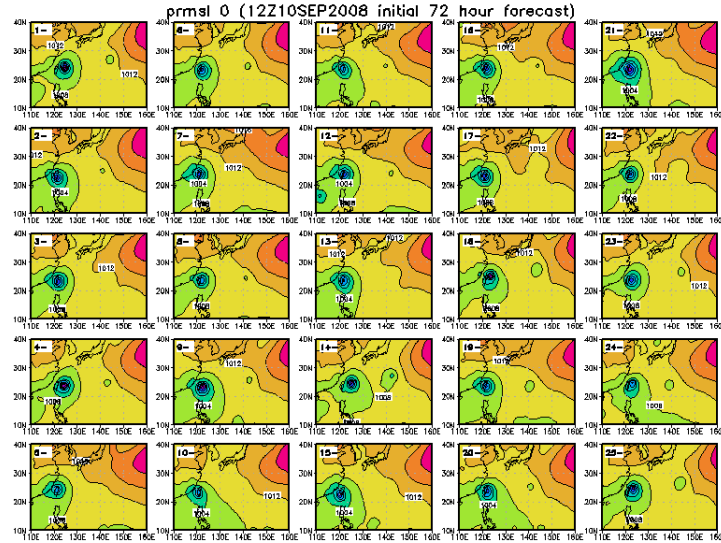


Figure 5 Sample of weekly ensemble forecasts at specific forecast times

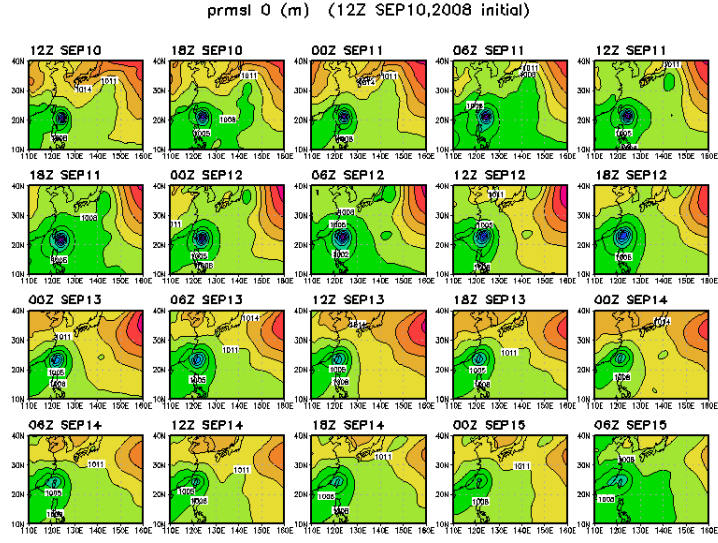


Figure 6 Sample of the time-series for the evolution of each member, the ensemble mean and the spread in the weekly ensemble forecast

### 3.3.2 Ensemble forecasts from JMA's typhoon model

The six-hourly ensemble forecasts from JMA's typhoon model are provided in the form of pictures and binary data.

There are three types of picture: those with all members at a specific forecast time; time-series representations for each member and the ensemble mean and spread; and ‘closer look’ representations. The first and second kinds are similar to those for weekly ensemble forecasts. The ‘closer look’ type is similar to these, but is zoomed in to focus on the TC center (Fig. 7).

These pictures are provided in individual month/initial time directories for each kind except for the closer-look type, which is provided in each TC directory. Binary data are provided in monthly directories.

T0813 prmsl 0 (12Z10SEP2008 initial 48h FCST)

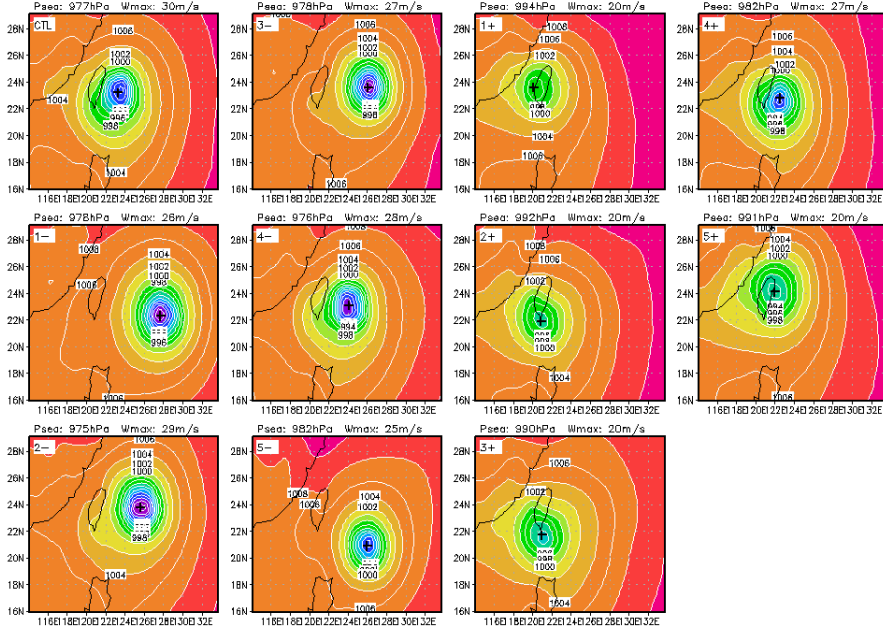


Figure 7 Sample ‘closer look’ pictures showing all 11 sets of member data for a specific forecast time

### 3.3.3 One-month ensemble forecasts

The results of one-month ensemble forecasts are provided in the form of pictures and binary data.

There are three kinds of picture: those with all members at a specific forecast time; time-series representations for each member and the ensemble mean and spread; and Hovmöller diagrams for each member and ensemble mean and spread (Fig. 8). The first and the second kinds are similar to those for weekly ensemble forecasts.

These pictures are made for mean sea level pressure, geopotential height at 500 hPa, wind speed, velocity potential (chi), divergence and vorticity at 850 hPa and 200 hPa. Binary data are individually provided for velocity potential (chi), pressure vertical velocity (omg), surface pressure (ps), mean sea level pressure (psea), stream function (psi), surface total precipitation (rain), temperature (t), temperature 2 m above ground level (ts), dew point depression (ttd), dew point depression 2 m above ground level (ttds), u wind (u), u wind 2 m above ground level (us), v wind (v), v wind 2 m above ground level (vs), vorticity (vor) and geopotential height (z).

Binary data are provided in each element directory for each initial time.

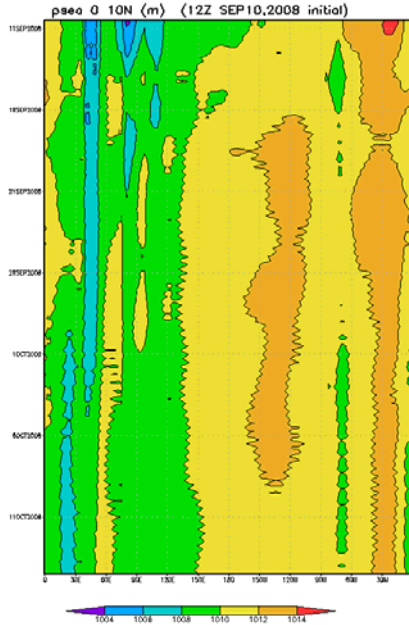


Figure 8 Sample Hovmöller diagram for a one-month ensemble forecast

### 3.3.4 Sensitivity analysis by JMA

Pictures of sensitivity analysis for the JAPAN, GUAM, TAIWAN and MVTY areas with one-day and two-day lead times are provided.

## 3.4 Satellite data

Gridded QuikSCAT data produced by Remote Sensing Systems are provided in GrADS format with control files. As mentioned in Section 2.3, the descending (ascending) passes are treated as 09 UTC (21 UTC) observations.

## 3.5 JMA in-situ data

### 3.5.1 Surface observation

Ten-second and one-minute observation data from JMA's network of observatories are provided in binary format (not GrADS format).

### 3.5.2 Radar data

Radar observation data are provided (not in GrADS format).

### 3.5.3 Upper-sounding data

Upper-sounding data from Ishigaki-jima, Minami-daitou-jima, Naze, Hachijo-jima and from the Chofu-maru and Seifu-maru research vessels are provided in text format.

#### *3.5.4 Wind profiler data*

Wind profiler data from JMA's wind profiler network (WINDAS) are provided (not in GrADS format).

#### **3.6 MTSAT-1R data**

Half-hourly MTSAT-1R IR1 (ir1), water vapor (wv), VIS (vs) and short-wave IR (ir4) channel TBB data are provided in GrADS format with control files and in SATAID format.

#### *3.7 Cyclone XML data*

Cyclone XML data (<http://www.bom.gov.au/bmrc/projects/THORPEX/TC/index.html>) are provided in original XML format and in parsed HTML format. Directories are prepared for each month.

### **Acknowledgement**

We would like to thank Dr. Mio Matsueda for assistance with data processing, Dr. Naoko Kitabatake for contribution to provision of the scripts, Dr. Kazuo Saito and Dr. Masaru Kunii for provision of mesoscale ensemble forecast outputs, and Mr. Shuji Nishimura for provision of Dvorak analysis data. We are also very grateful to all those involved in the T-PARC project.



# JMA's Five-day Tropical Cyclone Track Forecast

**Kenji KISHIMOTO**

Forecast Division, Forecast Department, Japan Meteorological Agency

## Abstract

Since 22 April 2009, the Japan Meteorological Agency (JMA) has issued five-day tropical cyclone (TC) track forecasts. This paper introduces these forecasts, including the method used, interpretation of the results obtained, forecast cases and future challenges. One of the forecast's unique aspects is its determination of the radius of a 70% probability circle (PC) using the level of forecast uncertainty based on the ensemble spread of JMA's Typhoon Ensemble Prediction System (TEPS).

## 1. Introduction

Since 22 April 2009, the Japan Meteorological Agency (JMA) has issued five-day tropical cyclone (TC) track forecasts to encourage early public attention to and preparation for TCs. The purpose of this paper is to introduce these forecasts. First, an overview is given in Section 2, and then the forecast method, interpretation of the results obtained and some sample forecast cases are described in Sections 3, 4 and 5, respectively. To conclude, future challenges are outlined in Section 6.

## 2. Overview of five-day TC track forecasts

Figure 1 shows a schematic representation of JMA's TC forecast issuance. First, the Agency issues three-day TC track and intensity forecasts about 50 minutes after the usual observation times (0050, 0650, 1250 and 1850 UTC). A five-day TC track forecast is then made for any TCs expected to maintain tropical storm (TS) intensity or higher over the next three days. This is issued about 40 minutes after the three-day forecast (0130, 0730, 1330 and 1930 UTC). If two or more named TCs exist at the same time, three-day and five-day forecasts for the second and subsequent TCs are issued about 70 minutes after the observation time (0110, 0710, 1310 and 1910 UTC) and about 40 minutes after the issuance of three-day forecasts (0150, 0750, 1350 and 1950 UTC), respectively. The five-day track forecast includes the center positions and radii of 70% probability circles (PCs) for the fourth and fifth days. The PC is a circular range into which a TC is expected to move with a probability of 70% at each valid time. TC intensity (central pressure, maximum sustained wind, peak gusts and storm warning area) is not predicted in five-day forecasts.

### 3. Method for five-day TC track forecasts

JMA makes five-day TC track forecasts mainly using outputs from the JMA typhoon ensemble prediction system (TEPS), which is run four times a day when there is a TC with TS intensity or higher (or one expected to reach such a level in the next 24 hours) in the area. The main specifications of TEPS are shown in Table 1. The system is explained in further detail by Yamaguchi and Komori (2009).

Figure 2 (a) shows a schematic representation of the forecast method. PCs for the fourth and fifth days are determined based on the distribution of TEPS ensemble members. The center of a PC is determined mainly using the mean position of these members. If they are divided clearly into two courses, the center does not represent the highest likelihood of the TC's position (see Figure 2 (b)). The size of a PC is determined mainly using the spread of TEPS ensemble members. Forecasters use products from TEPS as shown in Figure 3 as a measure of forecast uncertainty in order to determine the radius of a PC. Such circles show the latest status of forecast uncertainty, and are categorized into one of three groups (A, B and C) known as confidence levels. Once a forecaster determines the level of a forecast, the radius is automatically fixed through the conversion table from the confidence level to a PC radius prepared based on verification results from recent years (see Figure 4). Details of the categorization are given by Yamaguchi and Komori (2009).

### 4. Interpretation of five-day TC track forecasts

In five-day TC track forecasts, possible tracks are indicated using a distribution of PCs. Figure 5 illustrates some examples of possible tracks shown by such circles. Figure 5 (a) shows that a TC has a high chance of approaching the northern or eastern part of Japan within the next five days, while Figure 5 (b) indicates various possibilities, including a westward track to the Okinawa region and a northward track to mainland Japan.

### 5. Forecast cases

JMA conducted experimental operation of five-day TC track forecasts in autumn 2008. This section outlines the forecast results for two typhoons – Sinlaku (0813) and Jangmi (0815) – that formed in September and took similar courses. Section 5.1 explains their tracks, and Section 5.2 presents the forecast results.

#### 5.1 Tracks of Sinlaku (0813) and Jangmi (0815)

The best tracks of Sinlaku and Jangmi are shown in Figure 6. Sinlaku formed east of the Philippines at 18 UTC on 8 September. Moving northwestward, it approached the Okinawa Islands then Taiwan Island. After recurving north of Taiwan Island on 15 September, it moved east-northeastward over the East China Sea and transformed into an extratropical cyclone east of Japan. Jangmi formed east of the Philippines at 12 UTC on 24 September. Moving northwestward, it hit Taiwan Island. After recurving north of Taiwan Island on 29 September, it transformed into an extratropical cyclone south of Kyushu at 00 UTC on 1 October.

## 5.2 Forecast results

Figure 7 (a) shows three forecasts made for Sinlaku in one day from 18 UTC on 11 September. In the first forecast (the upper figure), the PC for the fifth day (the five-day PC) indicated that Sinlaku had a high chance of moving westward through Taiwan before hitting China. In the last one (the lower figure), the five-day PC generally covered the East China Sea, suggesting that it had a high chance of moving northeastward over the sea after recurving north of Taiwan. In this series of forecasts, the forecast tracks shown by the PC centers changed from northwestward to northeastward, while the sizes of the PCs themselves remained the same.

Figure 7 (b) shows forecasts made for Jangmi in one day from 06 UTC on 26 September. In the forecast track view showing only PC centers, the second forecast (the middle figure) seems quite different from the last one (the lower figure). On the other hand, the size of the five-day PC exhibited a large change. The one in the second forecast (the middle figure) was very large, indicating significant forecast uncertainty including the possibility of a northwestward track to China and an eastward track to Japan. In the final one (the lower figure), it shrunk to cover only the sea south of Japan, indicating a much higher chance of moving eastward to Japan and a lower likelihood of moving northwestward to China.

As shown in Jangmi's case, PC sizes for subsequent fourth and fifth days change depending on forecast uncertainty. It should be noted that possible TC tracks must be viewed not only in terms of PC centers but also in consideration of PC sizes.

## 6. Future challenges

With the extension of the forecast term from three to five days, one particular challenge needs to be addressed in the display of track forecasts. Figure 8 (a) shows the forecast for Nepartak (0919) at 06 UTC on 10 October 2009; the very large five-day PC indicated the possibility of its approaching mainland Japan. Figure 8 (b) shows the TEPS result used for this forecast; it indicates a very large spread from the northeastward and southwestward tracks and no chance of movement northwestward to the Japanese mainland – a scenario that could not be expressed using PCs. JMA will consider alternative methods such as an elliptical form instead of a circular form based on verification results over the next few years.

## References

Yamaguchi and Komori (2009): Outline of the Typhoon Ensemble Prediction System at the Japan Meteorological Agency, RSMC Tokyo - Typhoon Center Technical Review No. 11, 14-24.

<http://www.jma.go.jp/jma/jma-eng/jma-center/rsmc-hp-pub-eg/techrev/text11-2.pdf>

Table 1 Specifications of JMA's Typhoon Ensemble Prediction System (TEPS)

|                        |  |
|------------------------|--|
| Horizontal resolution  | 0.5625 deg. (60 km)  |
| Vertical resolution    | 60 unevenly spaced hybrid levels from the surface to 0.1 hPa |
| Forecast range         | 132 hours  |
| Initial time           | 00, 06, 12, 18 UTC   |
| Ensemble size          | 11 members (10 perturbed forecasts and 1 control forecast)   |
| Perturbation generator | Singular Vector (SV) method                                  |

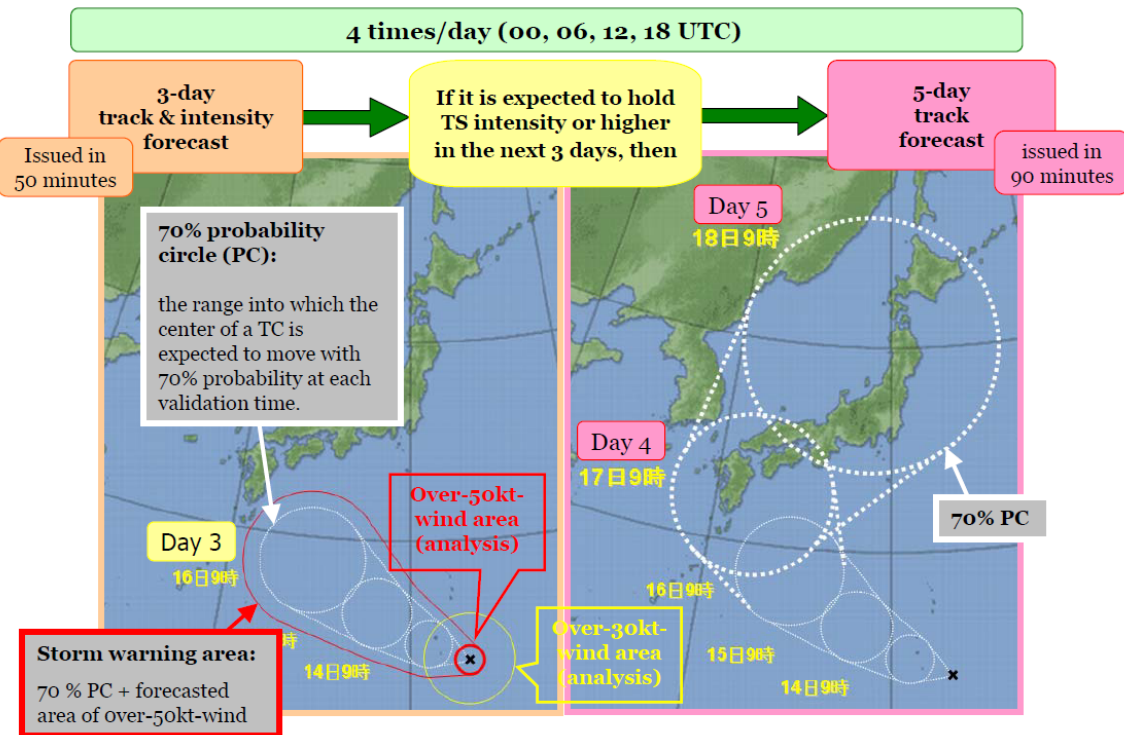


Figure 1 Issuance of JMA's TC forecast

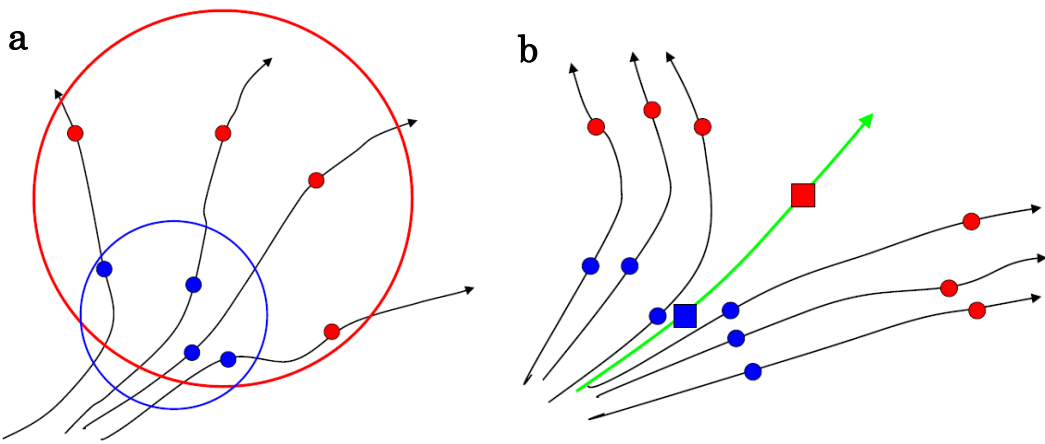


Figure 2 Five-day TC track forecast method. The circles show the 70% probability area, while the arrowed lines with circles and squares indicate member tracks and the ensemble mean track of TEPS, respectively.

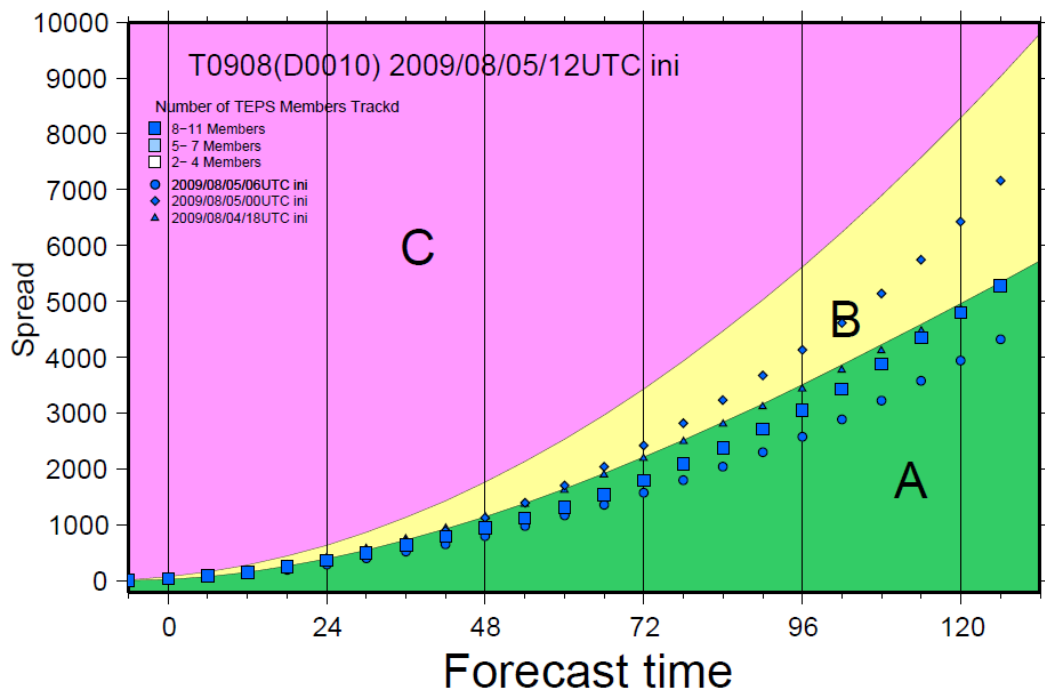


Figure 3 TEPS product on forecast uncertainty. The horizontal and vertical axes show the forecast time and the six-hourly accumulated TEPS ensemble spread, respectively.

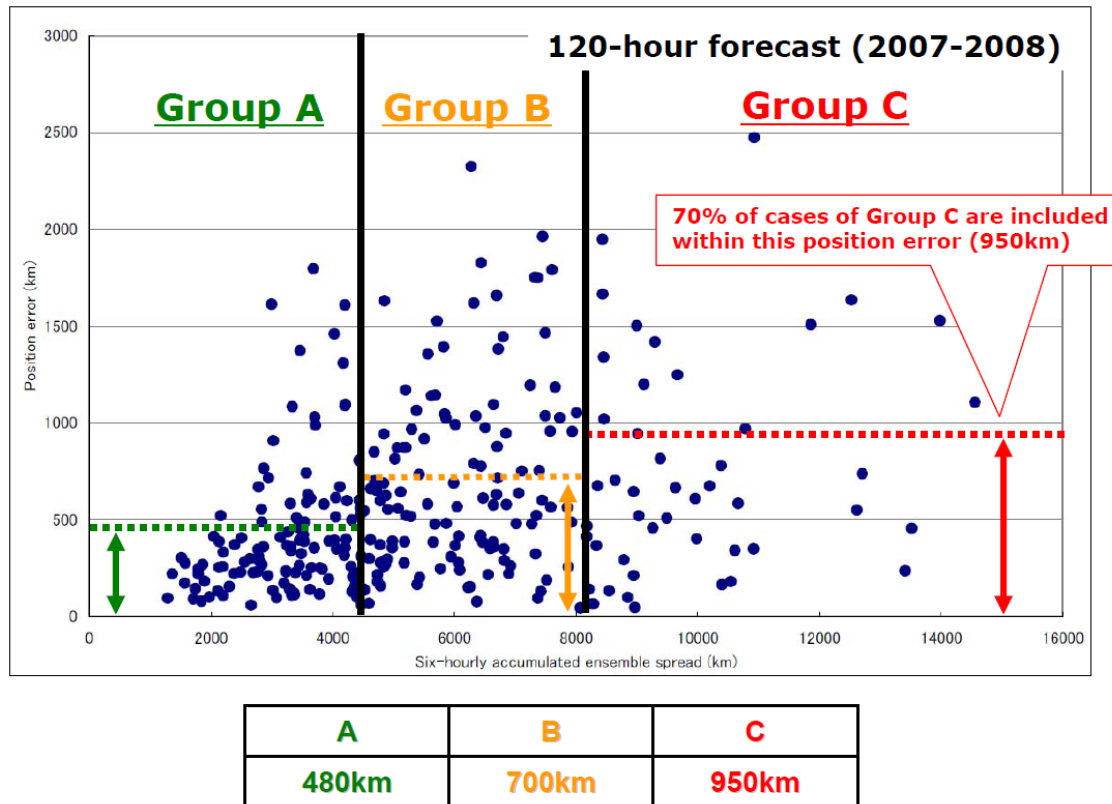


Figure 4 Verification results for each group (confidence level) from 2007 to 2008 (upper figure) and the conversion table from confidence level to PC radius as of 2009 (lower figure)

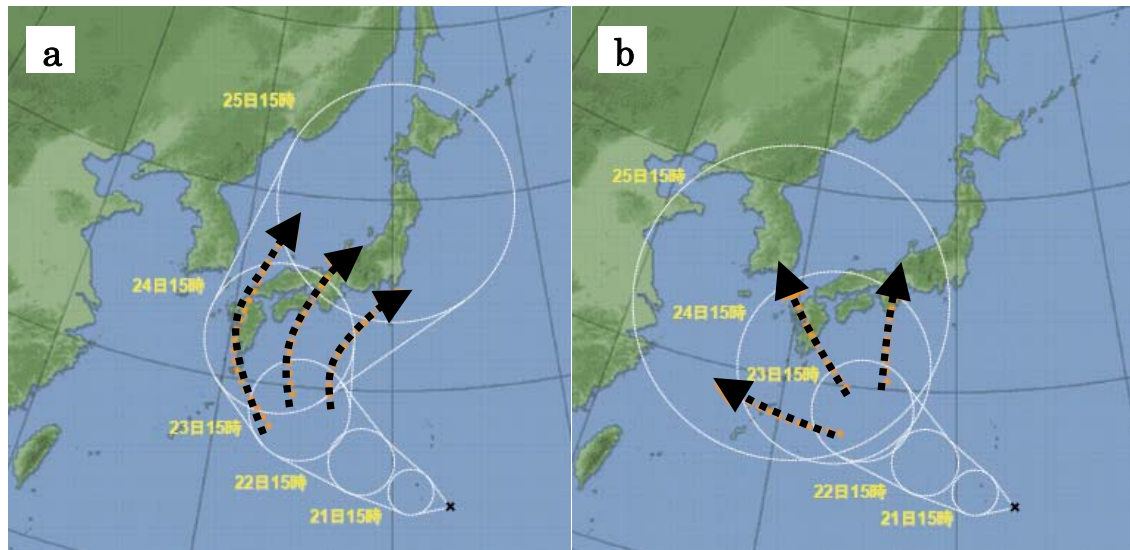


Figure 5 Examples of five-day track forecasts  
The dotted arrow lines indicate possible TC tracks.

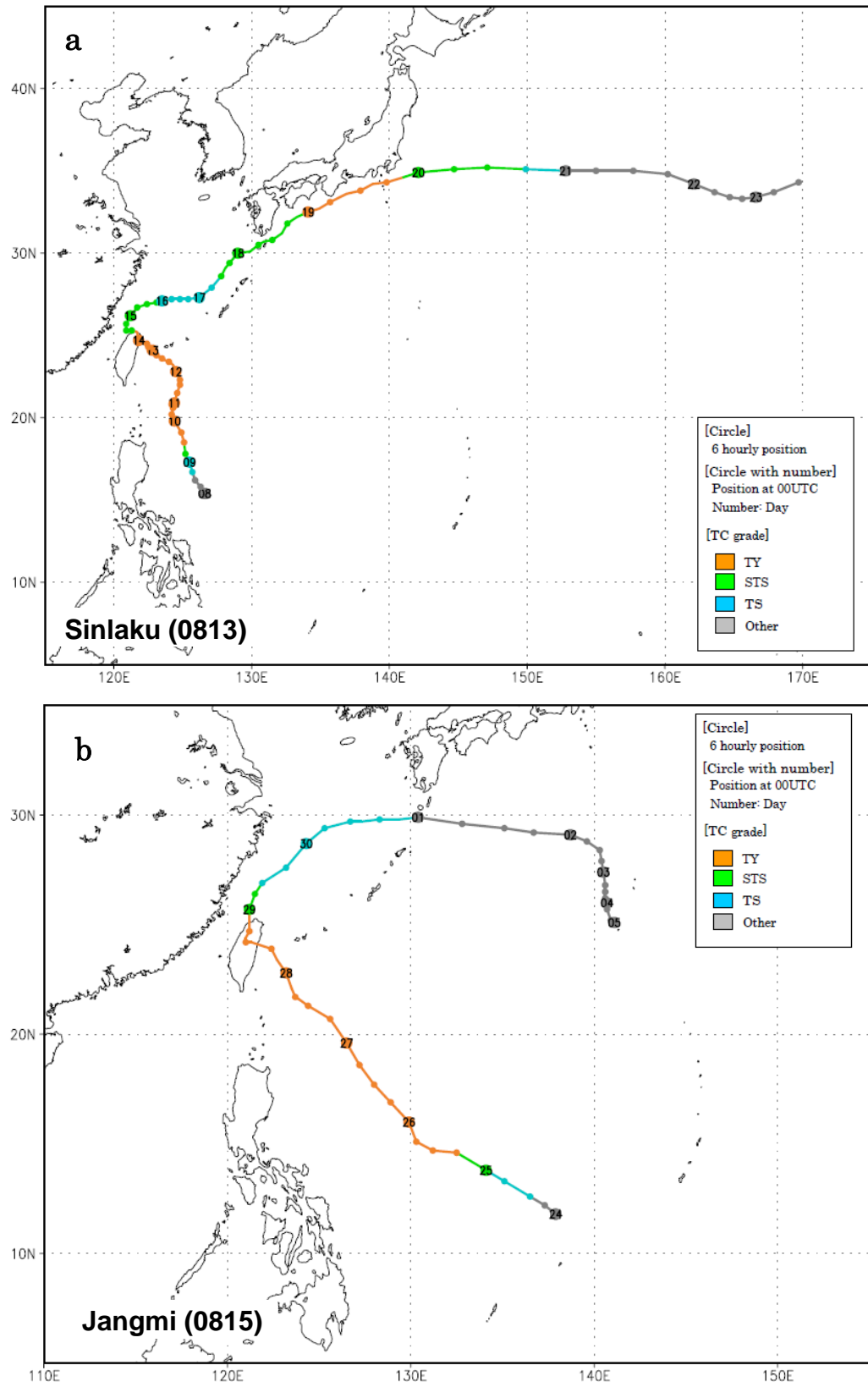


Figure 6 Tracks of a) Sinlaku (0813) and b) Jangmi (0815)

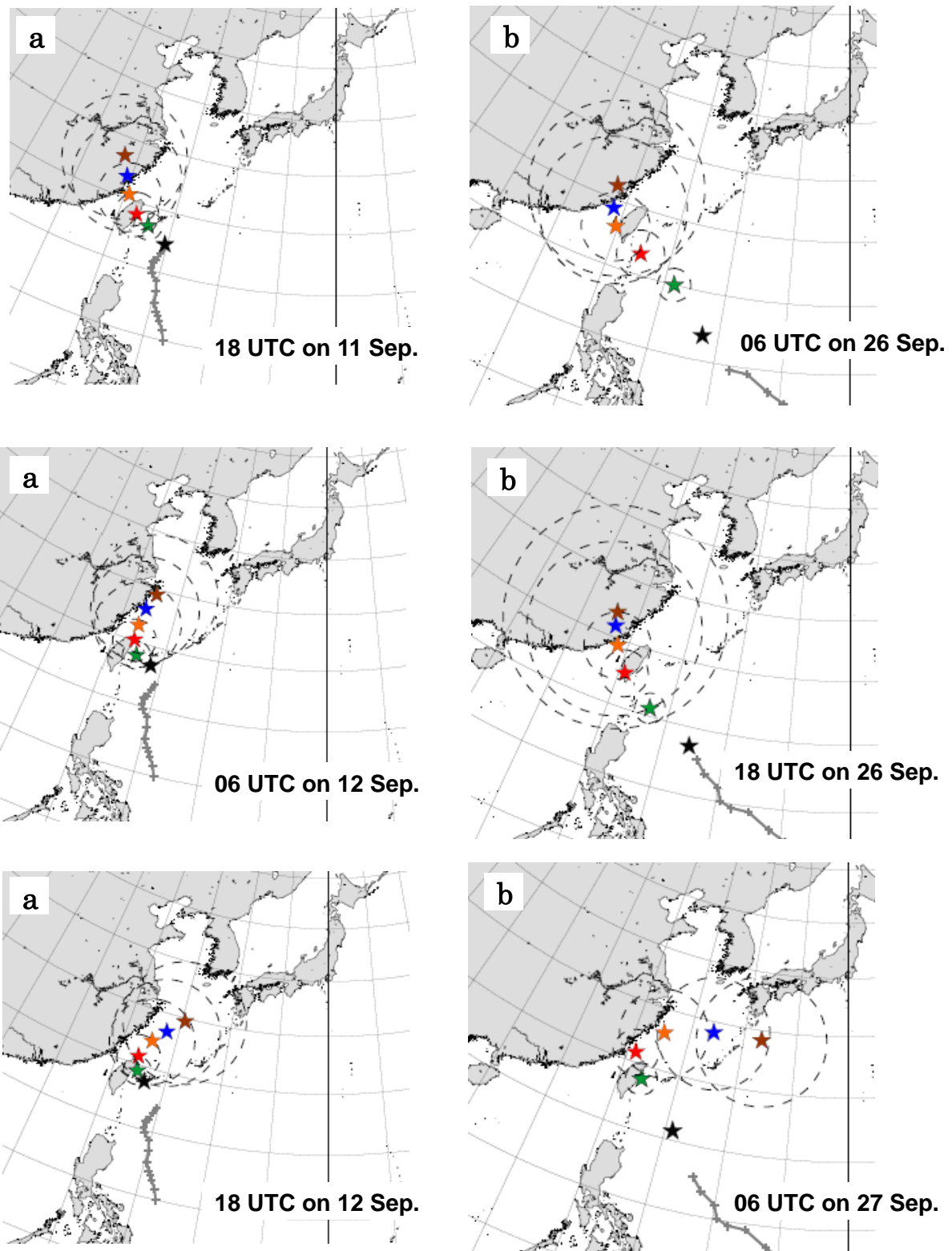


Figure 7 Forecast results for a) Sinlaku (0813) and b) Jangmi (0815)  
The stars show PC centers for the next one-to-five days.

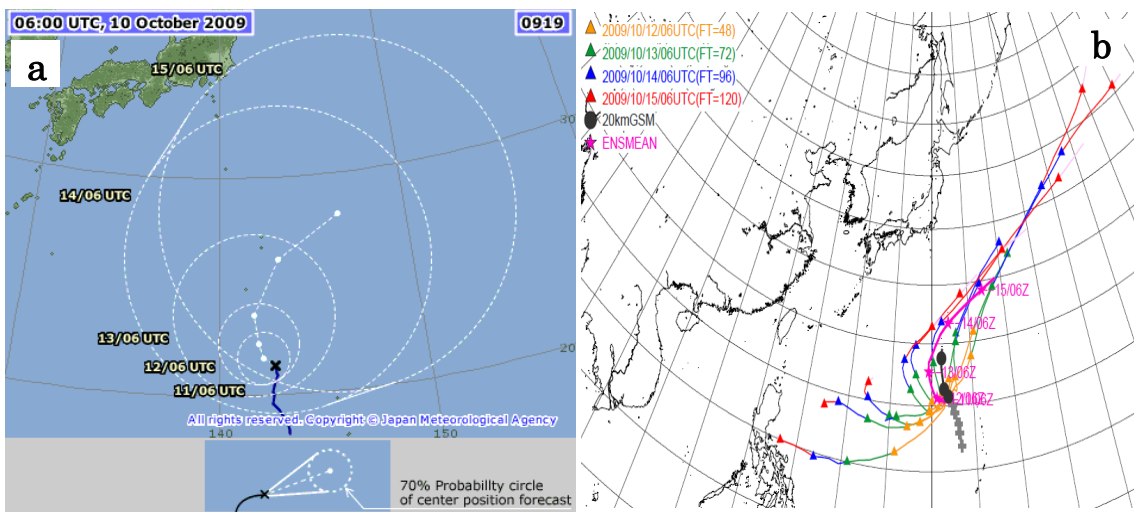


Figure 8 Five-day track forecast for Nepartak (0919)

Results of a) operational forecast at 06 UTC on 10 October 2009,  
and b) TEPS at the initial time of 00 UTC on 10 October 2009

**Japan Meteorological Agency**  
**1-3-4 Otemachi, Chiyoda-ku, Tokyo 100-8122, Japan**